© 2020. Published by The Company of Biologists Ltd | Journal of Cell Science (2020) 133, jcs241513. doi:10.1242/jcs.241513

RESEARCH ARTICLE

Regulation of intrinsic polarity establishment by a differentiation-type MAPK pathway in *S. cerevisiae*

Aditi Prabhakar, Jacky Chow*, Alan J. Siegel and Paul J. Cullen‡

ABSTRACT

All cells establish and maintain an axis of polarity that is critical for cell shape and progression through the cell cycle. A well-studied example of polarity establishment is bud emergence in the yeast *Saccharomyces cerevisiae*, which is controlled by the Rho GTPase Cdc42p. The prevailing view of bud emergence does not account for regulation by extrinsic cues. Here, we show that the filamentous growth mitogen activated protein kinase (fMAPK) pathway regulates bud emergence under nutrient-limiting conditions. The fMAPK pathway regulated the expression of polarity targets including the gene encoding a direct effector of Cdc42p, Gic2p. The fMAPK pathway also stimulated GTP-Cdc42p levels, which is a critical determinant of polarity establishment. The fMAPK pathway activity was spatially restricted to bud sites and active during the period of the cell cycle leading up to bud emergence. Time-lapse fluorescence microscopy showed that the fMAPK pathway stimulated the rate of bud emergence during filamentous growth. Unregulated activation of the fMAPK pathway induced multiple rounds of symmetry breaking inside the growing bud. Collectively, our findings identify a new regulatory aspect of bud emergence that sensitizes this essential cellular process to external cues.

KEY WORDS: Bud emergence, Cdc42p, Polarity establishment, MAPK, Pseudohyphal growth, Symmetry breaking

INTRODUCTION

All cells establish an axis of polarity, which is critical for cell shape, the organization of cellular compartments and progression through the cell cycle (Doerr and Ragkousi, 2019). Cell polarity can be reorganized in response to intrinsic and extrinsic cues and is required during development and for other processes that require dynamic changes in cell shape such as cell migration and differentiation (Henderson et al., 2018; Pei et al., 2019; Piroli et al., 2019). Defects in cell polarity are commonly associated with human disease. For example, the mis-regulation of cell polarity leads to metastasis in many types of cancers (Fomicheva et al., 2020; Noguchi et al., 2018; Taciak et al., 2018).

Cdc42p and other members of the Rho family of GTPases are central regulators of cell polarity (Arkowitz and Iglesias, 2008; Irazoqui and Lew, 2004; Jimeno and Santos, 2017; Pringle et al., 1995; Pruyne and Bretscher, 2000a,b; Woods and Lew, 2019; Zihni and Terry, 2015). In the yeast *Saccharomyces cerevisiae*, Cdc42p regulates bud emergence, which is an essential process where daughter cells or buds are produced from mother cells. The pathway that regulates bud emergence has been extensively studied and represents one of the best examples for how cells establish an axis of polarity (Fig. 1A, green pathway). Activation of Cdc42p by the guanine nucleotide exchange factor (GEF) Cdc24p at bud sites – or at random sites in bud-site-selection mutants – results in symmetry breaking, which commits the cell to grow at a particular site. Positive and negative feedback loops promote polarity establishment by amplifying the levels of active or GTP-bound Cdc42p at the incipient bud site (Chiou et al., 2018; Irazoqui et al., 2003; Kozubowski et al., 2008; Woods and Lew, 2019). The GTP-bound conformation of Cdc42p binds effector proteins (Bendezú and Martin, 2013; Guo et al., 2010; McCormack et al., 2013; Wu and Jiang, 2005; Wu et al., 2006; Yang et al., 2007), including Gic1p and Gic2p (Brown et al., 1997; Chen et al., 1997; Iwase et al., 2006; Kawasaki et al., 2003; Liu et al., 2019), p21 activated kinases (PAKs) Ste20p and Cla4p (Cvrckova et al., 1995; Gulli et al., 2000; Hofmann et al., 2004; Simon et al., 1995; Takahashi and Pryciak, 2007), and the formin Bni1p (Evangelista et al., 1997; Sherer et al., 2018). In a highly choreographed manner that is coordinated with the cell cycle (Moran et al., 2019), effector proteins regulate the assembly of the septin ring, which forms a diffusion barrier between mother and daughter cells, and the formation of actin cables, which direct the delivery of vesicles to the nascent bud site. In this way, buds are produced from mother cells in a precisely spatially and temporally regulated manner.

Cdc42p also regulates MAPK pathways (Brown et al., 1996; Martin, 2019; Simon et al., 1995). MAPK pathways are evolutionarily conserved signaling modules that control cell differentiation and the response to stress in eukaryotes (Dinsmore and Soriano, 2018; Papa et al., 2019; Raman et al., 2007; Yoon and Seger, 2006). In yeast, nutrient limitation induces a Cdc42p-dependent MAPK pathway that regulates filamentous/invasive/pseudohyphal growth [Fig. 1A, blue pathway, fMAPK pathway (Adhikari et al., 2015; Borneman et al., 2007; Cullen, 2015; Gancedo, 2001; Gimeno et al., 1992; Leberer et al., 1997; Mösch et al., 1999; Mosch et al., 1996; Pan et al., 2000; Peter et al., 1996; Roberts and Fink, 1994)]. Filamentous growth occurs in many fungal species, and in some plant and animal pathogens, filamentous growth is required for virulence (Desai et al., 2014; Lagree and Mitchell, 2017; Lo et al., 1997). At the head of the fMAPK pathway, plasma membrane proteins Msb2p and Sho1p regulate the Cdc42p module, which leads to the recruitment and activation of Ste20p, the specific Cdc42p effector that regulates the fMAPK pathway. Ste20p in turn induces a MAPK cascade composed of Ste11p (MAPKKK), Ste7p (MAPKK) and Kss1p (MAPK) (Madhani et al., 1997; Roberts and Fink, 1994). MAPK Kss1p regulates the activity of transcription factors Ste12p and Tec1p, as well as transcriptional repressors and other factors (Bardwell et al., 1998; Madhani and Fink, 1997;

Department of Biological Sciences, University at Buffalo, Buffalo, NY 14260-1300, USA.
*Present address: Department of Immunology, Roswell Park Comprehensive Cancer Center, Buffalo, NY 14263, USA.

‡Author for correspondence (pjcullen@buffalo.edu)

P.J.C., 0000-0002-6703-1480

Received 7 November 2019; Accepted 12 February 2020

Journal of Cell Science (2020) 133, jcs241513. doi:10.1242/jcs.241513

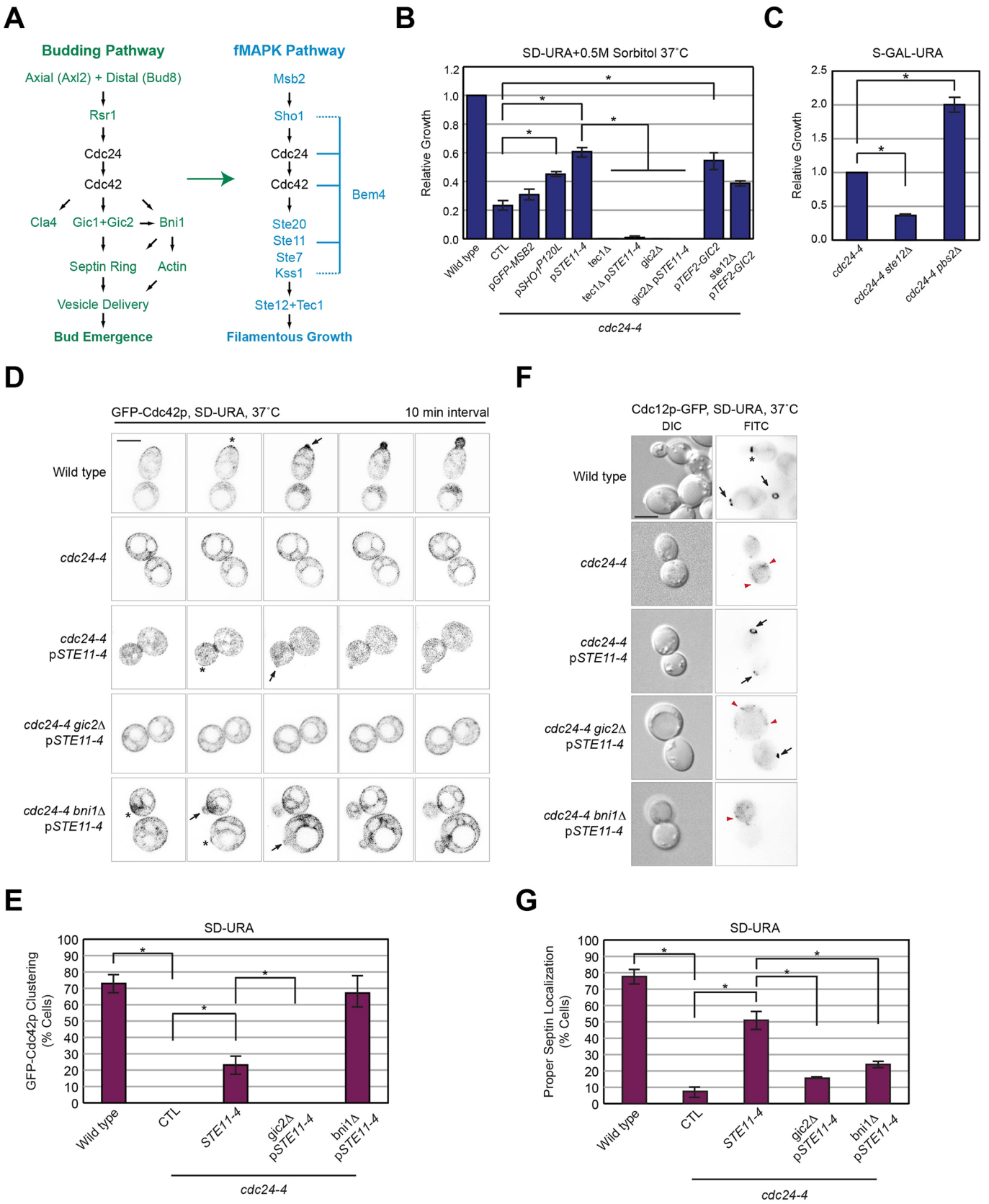

Fig. 1. See next page for legend.

van der Felden et al., 2014) to regulate expression of target genes that bring about the filamentous cell type (Roberts et al., 2000; Rupp et al., 1999).

Despite the fact that bud emergence is extensively regulated by positive and negative feedback loops and is coordinated with the cell cycle, bud emergence is not known to be regulated by extrinsic

Journal of Cell Science (2020) 133, jcs241513. doi:10.1242/jcs.241513

Fig. 1. Role of the fMAPK pathway in rescuing the growth defect of the *cdc24-4* mutant. (A) Pathways that regulate bud emergence (green) and filamentous growth (blue). Cdc24p and Cdc42p regulate both pathways. Not all proteins are shown. (B) Growth of the indicated strains relative to wild-type cells. p*GFP-MSB2*, p*SHO1*^{P120L}, p*STE11-4* and p*TEF2-GIC2* were expressed from plasmids (see Table S2) in the indicated strains (see Table S1). Error bars show the standard error of the mean (s.e.m.) for three separate trials. **P*<0.01. CTL, plasmid pRS316. (C) Growth of strains relative to the *cdc24-4* mutant. This experiment was performed in galactose (GAL) medium, which also compromised the viability of the *cdc24-4* mutant, because the *pbs2*Δ mutant has a growth defect at 37°C (Winkler et al., 2002). (D) Inverted maximum intensity projection of GFP-Cdc42p localization in the indicated strains, examined after incubation at 37°C for 4 h. *GFP-Cdc42p clustering. Arrows, sites of bud emergence. Scale bar, 5 µm. (E) Quantification of GFP-Cdc42p clustering. Error bars, s.e.m. for three separate trials. At least 50 cells were counted in each trial. **P*<0.05. (F) Cdc12p-GFP localization in the indicated strains, examined after incubation at 37°C for 4 h. Black arrows, Cdc12p-GFP localization in incipient buds; *Cdc12p-GFP localization at mother-bud neck in growing bud; red arrowheads, mislocalized Cdc12p-GFP. Scale bar, 5 µm. (G) Quantification of septin localization; see panel 1E for details.

cues or signaling pathways. The fMAPK and polarity pathways both require Cdc42p, which suggests that functional cross-talk may occur between the two pathways. In support of this possibility, we have recently found that bud-site-selection proteins regulate the fMAPK pathway [Fig. 1A, green arrow (Basu et al., 2016)]. We tested the hypothesis that reciprocal cross-talk might occur from the fMAPK pathway to the bud emergence pathway, and discovered a role for the fMAPK pathway in regulating bud emergence. An active fMAPK pathway rescued the bud emergence defect of a polarity mutant (*cdc24-4*), and was required for proper bud emergence during filamentous growth. The fMAPK pathway accomplished this role by inducing expression of a direct effector of Cdc42p that functions in budding (*GIC2*) and by directly stimulating GTP-Cdc42p levels. The activity of the fMAPK pathway was regulated during the cell cycle to peak prior to and during bud emergence and when mis-regulated induced growth at multiple sites. Our study therefore identifies a new regulatory facet of bud emergence that is subject to regulation by a MAPK pathway and external cues. Given that Rho GTPases are functionally connected to MAPK pathways in higher eukaryotes, polarity establishment might be generally regulated by MAPK and other pathways.

RESULTS

The fMAPK pathway rescues the bud emergence defect of *cdc24-4* through Gic2p

Multicopy Suppressor of Budding Defect 2 (*MSB2*) was initially characterized as a high-copy suppressor of the budding and growth defects of the *cdc24-4* mutant (Bender and Pringle, 1989, 1992). Msb2p was subsequently identified as the mucin-type glycoprotein that regulates the fMAPK pathway [Fig. 1A, blue pathway (Cullen et al., 2004)]. To determine whether Msb2p regulates budding through the fMAPK pathway, plasmids carrying alleles that hyperactivate the fMAPK pathway were introduced into the *cdc24-4* mutant and examined for growth at 37°C, in synthetic medium lacking uracil to maintain selection for the plasmids, and supplemented with 0.5 M sorbitol, which stabilizes cell integrity (Bender and Pringle, 1989, 1992). Insertion of Green Fluorescent Protein (GFP) into the extracellular domain of Msb2p results in a version of the protein that hyperactivates the fMAPK pathway (Adhikari et al., 2015; Vadaie et al., 2008). p*GFP-MSB2* weakly suppressed the growth defect of the *cdc24-4* mutant (Fig. 1B). Hyperactive versions of Sho1p (p*SHO1*^{P120L}) and Ste11p (p*STE11-4*) more robustly rescued the growth defect of the *cdc24-4* mutant (Fig. 1B). p*STE11-4* also rescued the polarity defect of the *cdc24-4* mutant (Fig. S1A) and was used for most of the subsequent experiments. Therefore, activated versions of MAPK pathway components can rescue the growth and polarity defects of a bud emergence mutant.

Msb2p, Sho1p and Ste11p regulate two MAPK pathways [fMAPK and high-osmolarity glycerol response (HOG) (Saito, 2010)]. A pathway-specific regulator of the HOG pathway, Pbs2p (Brewster et al., 1993; Nishimura et al., 2016; Zarrinpar et al., 2004), was not required for growth of the *cdc24-4* mutant (Fig. 1C). In fact, the *cdc24-4*Δ *pbs2*Δ double mutant grew better than the *cdc24-4* single mutant, perhaps because the HOG pathway negatively regulates the fMAPK pathway and its loss results in hyperactive fMAPK pathway activity (Davenport et al., 1999). By comparison, a pathway-specific regulator of the fMAPK pathway, Tec1p (Madhani and Fink, 1997), was required for viability of the *cdc24-4* mutant (Fig. 1B). Tec1p functions with another transcription factor, Ste12p (Liu et al., 1993), which was also required for growth of *cdc24-4* (Fig. 1C). Ste11p and Ste12p also regulate the mating pathway, but these experiments were carried out in a mating defective strain (*ste4*Δ). Tec1p was required for suppression of the growth defect of the *cdc24-4* mutant by p*STE11-4* (Fig. 1B). p*STE11-4* also induced phosphorylation of the MAP kinase for the fMAPK pathway, Kss1p (P∼Kss1p) in the *cdc24-4* mutant (Fig. S1B). Therefore, the MAPK pathway that controls filamentous and invasive growth regulates bud emergence in a defined genetic context.

The fMAPK pathway controls filamentous growth by regulating target genes that control cell adhesion [*FLO11* (Rupp et al., 1999)], bud-site selection [*BUD8* (Cullen and Sprague, 2002; Harkins et al., 2001; Taheri et al., 2000)] and cell elongation [*CLN1* (Kron et al., 1994; Loeb et al., 1999; Madhani et al., 1999)]. None of these genes was required for viability of the *cdc24-4* mutant (Fig. S1C). To identify relevant polarity targets of the fMAPK pathway, gene ontology (GO) term analysis was performed on data generated in Chow et al. (2019). Polarity targets of the fMAPK pathway included genes that regulate bud-site selection (Fig. S1D; *AXL2*, *BUD8*, *RSR1* and *RAX2*), polarity establishment (*MSB2*, *GIC2* and *RGA1*), and septin ring organization (*GIC2*, *AXL2* and *RGA1*). We explored the roles of many of these genes in this study. We started with *GIC2*, which encodes a direct effector of Cdc42p that along with *GIC1* functions in bud emergence [Fig. 1A, green (Brown et al., 1997; Chen et al., 1997)]. The *GIC2* gene was a target of the fMAPK pathway (Fig. S1E; see also MacIsaac et al., 2006).

Gic2p was required for viability of the *cdc24-4* mutant (Fig. 1B; Costanzo et al., 2010) and to suppress the growth defect of *cdc24-4* by p*STE11-4* (Fig. 1B). Expression of *GIC2* from a fMAPK pathway-independent promoter partly rescued the growth defect of the *cdc24-4* mutant (Fig. 1B; p*TEF2-GIC2*) even in cells lacking an intact fMAPK pathway (p*TEF2-GIC2 ste12*Δ). *GIC1* was not a target of the fMAPK pathway (Fig. S1E) and p*STE11-4* suppressed the *cdc24-4 gic1*Δ mutant better than *cdc24-4 gic2*Δ (Fig. S1F). Thus, Gic2p is a target of the fMAPK pathway that is required for fMAPK pathway-dependent rescue of the *cdc24-4* mutant.

Gic proteins regulate clustering or polarization of Cdc42p at bud sites (Daniels et al., 2018; Kang et al., 2018), which is a critical step in polarity establishment. Time-lapse fluorescence microscopy was performed to examine the viability of the *cdc24-4* mutant on SD-URA media. This approach showed that GFP-Cdc42p clustered at a specific site on the cell cortex (Fig. 1D; wild-type, asterisk), from which site new buds emerged. The *cdc24-4* mutant was defective for GFP-Cdc42p clustering and bud emergence (Fig. 1D; *cdc24-4*). Analysis of 30 cells showed this difference to be

Journal of Cell Science (2020) 133, jcs241513. doi:10.1242/jcs.241513

statistically significant (Fig. 1E). p*STE11-4* partially restored GFP-Cdc42p clustering and bud emergence to the *cdc24-4* mutant (Fig. 1D,E). Rescue of bud emergence by p*STE11-4* was dependent on Gic2p (Fig. 1D,E).

During bud emergence, Gic proteins also regulate formation of the septin ring (Bi and Park, 2012; Iwase et al., 2006; Kang et al., 2018; Okada et al., 2013; Sadian et al., 2013). In wild-type cells, the septin Cdc12p-GFP was localized in a ring prior to bud emergence (Fig. 1F; black arrows) and to the mother-bud neck in budding cells (Fig. 1F; asterisk). In the *cdc24-4* mutant, Cdc12p-GFP showed a punctate pattern on the cell cortex (Fig. 1F; red arrowheads). Based on the analysis of over 150 cells, the localization defect was statistically significant (Fig. 1G). p*STE11-4* partially rescued the septin localization defect of the *cdc24-4* mutant (Fig. 1F,G), which was dependent on Gic2p (Fig. 1F,G). The fMAPK pathway did not suppress the growth and morphological defects of the *cdc12-6* mutant and septin kinase mutants, *elm1*Δ and *gin4*^{G377T}, which indicates that the pathway functions upstream of the septins themselves (Fig. S2). Gic2p also promotes the interaction between Cdc42p and Bni1p (Chen et al., 2012). Bni1p was not required for GFP-Cdc42p clustering or bud emergence (Fig. 1E,F) but was required for septin localization in the *cdc24-4* mutant (Fig. 1F,G). Bni1p is required for septin ring assembly (Gladfelter et al., 2005; Kadota et al., 2004). In wild-type cells, Gic2p was required for invasive growth (plate-washing assay; Fig. S3A), colony ruffling (Fig. S3B) and septin organization (Fig. S3C–E) of filamentous cells. Gic2p did not regulate the fMAPK pathway (Fig. S3F). These results establish a new role for the fMAPK pathway in regulating bud emergence by a mechanism that involves the regulated expression of Gic2p. In the next section, we examine the role of the fMAPK pathway in regulating bud emergence in wild-type cells, under conditions of filamentous growth.

The fMAPK pathway regulates GTP-Cdc42p levels during filamentous growth

Like other monomeric GTPases, the exchange of GDP for GTP alters the conformation of Cdc42p and allows the protein to bind effector proteins. During budding, the increase in GTP-Cdc42p levels is critical for symmetry breaking and polarity establishment (Irazoqui et al., 2003; Kozubowski et al., 2008). Msb2p interacts with GTP-Cdc42p to activate the fMAPK pathway (Cullen et al., 2004). During filamentous growth, the level and activity of Msb2p is stimulated by positive feedback (Fig. S1D). To test whether Msb2p and the fMAPK pathway affect the levels of GTP-Cdc42p in the cell, a fluorescent reporter that measures GTP-Cdc42p levels was examined [Gic2p-PBD-tdTomato (Okada et al., 2013)]. Compared with cells undergoing yeast-form growth (YEPD), cells undergoing filamentous growth showed elevated levels of GTP-Cdc42p (Fig. 2A; YEP-GAL). The increase in GTP-Cdc42p levels was dependent on the fMAPK pathway (Fig. 2A) in a manner that was statistically significant (Fig. 2B; YEP-GAL; P<0.00001). As previously shown (Okada et al., 2013), the level of GTP-Cdc42p was also higher in cells responding to the mating pheromone α-factor (Fig. 2A,B). In this case, the increase was independent of the fMAPK pathway.

One caveat in interpreting the above results is that *GIC2-PBD*-tdTomato is driven by its endogenous promoter, which, as shown above, is regulated by the fMAPK pathway. As a separate test, the activity of a Cdc42p biosensor (Smith et al., 2013) was examined by fluorescence lifetime imaging [FLIM-FRET (Sun et al., 2011)]. In wild-type cells, the Cdc42p biosensor exhibited shorter lifetimes with a version that mimics the GTP-bound conformation (Fig. 2C; Cdc42p^{Q61L}) and longer lifetimes with a version that mimics the GDP-bound conformation (Fig. 2C; Cdc42p^{D57Y}). Activation of the fMAPK pathway reduced the lifetime of the biosensor (Fig. 2C; *MSB2*$^{\Delta 100\text{-}818}$). This change corresponded to a 25% increase in the total levels of GTP-Cdc42p, which has previously been shown to

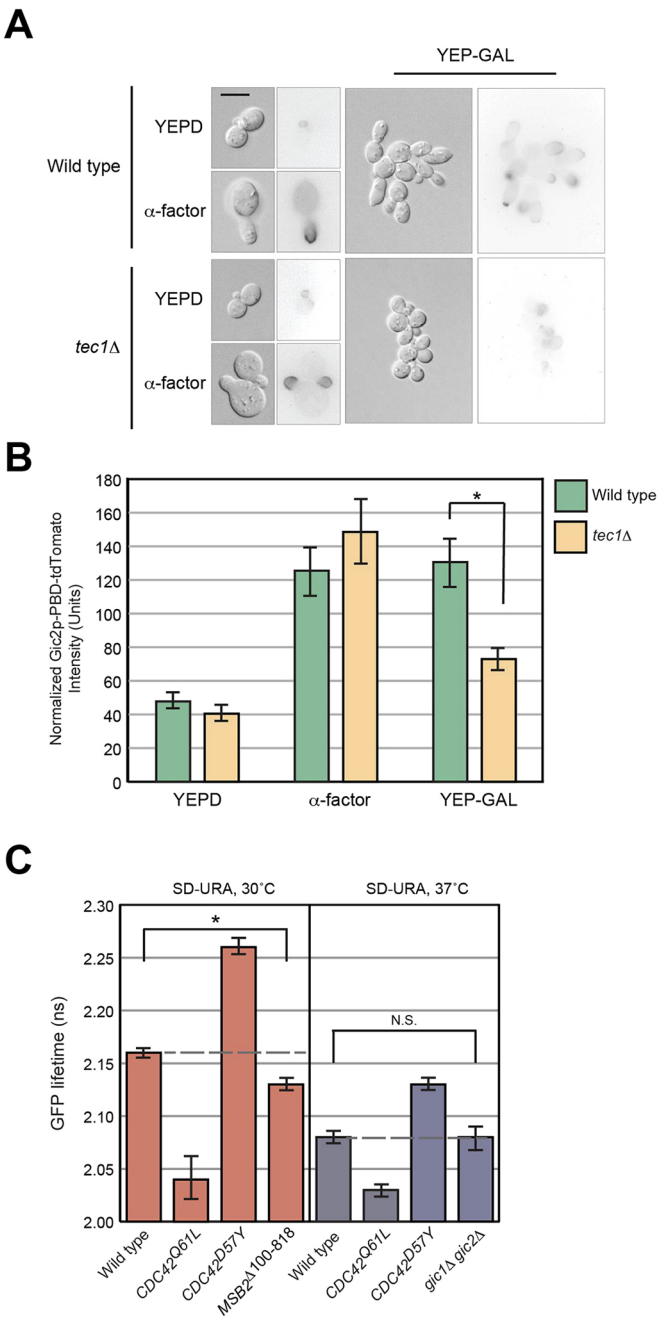

Fig. 2. Role of the fMAPK pathway in regulating GTP-Cdc42p levels at sites of bud emergence. (A) Localization of Gic2p-PBD-tdTomato in wild-type cells and the *tec1*Δ mutant under the indicated conditions. Micrographs were taken at the same exposure. Scale bar, 7.5 µm. (B) Quantitation of normalized total pixel intensity of Gic2p-PBD-tdTomato cluster in wild-type cells and the *tec1*Δ mutant (n>60). Error bars represent s.e.m.; *P<0.00001. (C) Wild-type cells and combinations of *MSB2*$^{\Delta 100\text{-}818}$ expressing plasmid-borne Cdc42p biosensors were examined by FLIM-FRET microscopy. In a separate experiment, wild-type cells and the *gic1*Δ *gic2*Δ double mutant expressing the wild-type Cdc42p biosensor were examined by FLIM-FRET microscopy after a 4 h shift at 37°C (n>15 cells from three trials). Error bars represent the s.e.m.; *P<0.05; N.S., not significant.

Journal of Cell Science (2020) 133, jcs241513. doi:10.1242/jcs.241513

reflect changes in Cdc42p activity during bud emergence (Smith et al., 2013). Cdc42p activity can also be affected by the Gic proteins (Daniels et al., 2018; Kang et al., 2018; Kawasaki et al., 2003) but the lifetime of the biosensor was not altered in the *gic1*Δ *gic2*Δ double mutant (Fig. 2C). Hyperactive versions of Msb2p, Sho1p and Ste11p also partially suppressed the growth defect of the *gic1*Δ *gic2*Δ double mutant at 37°C (Fig. S3G; Gandhi et al., 2006), which supports a role for fMAPK in regulating bud emergence that is separate from Gic protein function.

The fMAPK pathway is temporally and spatially regulated to coincide with bud emergence

Bud emergence occurs in the G_1 phase of the cell cycle (Gulli et al., 2000; Hartwell et al., 1970; Howell and Lew, 2012; Lew and Reed, 1993; Moran et al., 2019; Pringle et al., 1995). Whether the fMAPK pathway is active in the G_1 phase of the cell cycle has not been explored. To address this question, cells were synchronized in the G_1 phase of the cell cycle by α-factor (Breeden, 1997), and fMAPK pathway activity was assessed under basal (YEPD) and activating conditions (YEP-GAL) as cells progressed through the cell cycle. An epitope-tagged cyclin, Clb2p-HA, showed the expected pattern of cell-cycle regulation (Cepeda-García, 2017; Cross et al., 2005; Eluere et al., 2007; Irniger et al., 1995; Kuczera et al., 2010; Richardson et al., 1992; Wäsch and Cross, 2002), increasing after α-factor release by 60 min and decreasing by 90 min as cells entered anaphase (Fig. 3A; α-HA). P∼Kss1p levels also increased after α-factor release by 80 min and peaked by 100 min (Fig. 3A; P∼Kss1p). By comparison, the level of P∼Fus3p, which is the MAP kinase that regulates the mating pathway, decreased after release from α-factor (Fig. 3A; P∼Fus3p). Conditions that activate the fMAPK pathway (YEP-GAL) led to a delay in Clb2p-HA accumulation (Leitao and Kellogg, 2017) and also showed an increase in P∼Kss1p levels after the G_2/M phase of the cell cycle, prior to the next round of bud emergence (Fig. 3B). These results demonstrate that the activity of the fMAPK pathway is cell-cycle regulated and increases prior to and during bud emergence.

Bud emergence is spatially regulated in that it results from Cdc42p activation at bud sites (Caviston et al., 2003; Das et al., 2007; Freisinger et al., 2013; Okada et al., 2013). We previously showed that bud-site-selection proteins regulate the fMAPK pathway (Basu et al., 2016), which indicates that the fMAPK pathway is active at sites where bud emergence occurs. In line with this possibility, key regulators of the fMAPK pathway, including Sho1p (see below) and Ste20p are recruited to bud sites prior to bud initiation (Moran et al., 2019). Moreover, polarity targets of the fMAPK pathway included proteins that promote budding at bud sites (Fig. S1D). Polarity targets also included proteins that prevent budding at previous division sites or cytokinesis remnants. These included Rga1p (Fig. S1D), which along with other GTPase activating proteins (GAPs) prevents budding within the existing growth site (Kadota et al., 2004; Miller et al., 2017; Tong et al., 2007), and Rax2p (Fig. S1D), which restricts budding at previous division sites in a complex with Rax1p, Gps1p, Nba1p and Nis1p (Meitinger et al., 2014). Rga1p has been shown to negatively regulate the fMAPK pathway (Smith et al., 2002). Because these were negative regulators of the fMAPK pathway, cells were examined under pathway basal conditions (YEPD). Cells lacking Rax2p, Nba1p or Gps1p also showed elevated fMAPK pathway

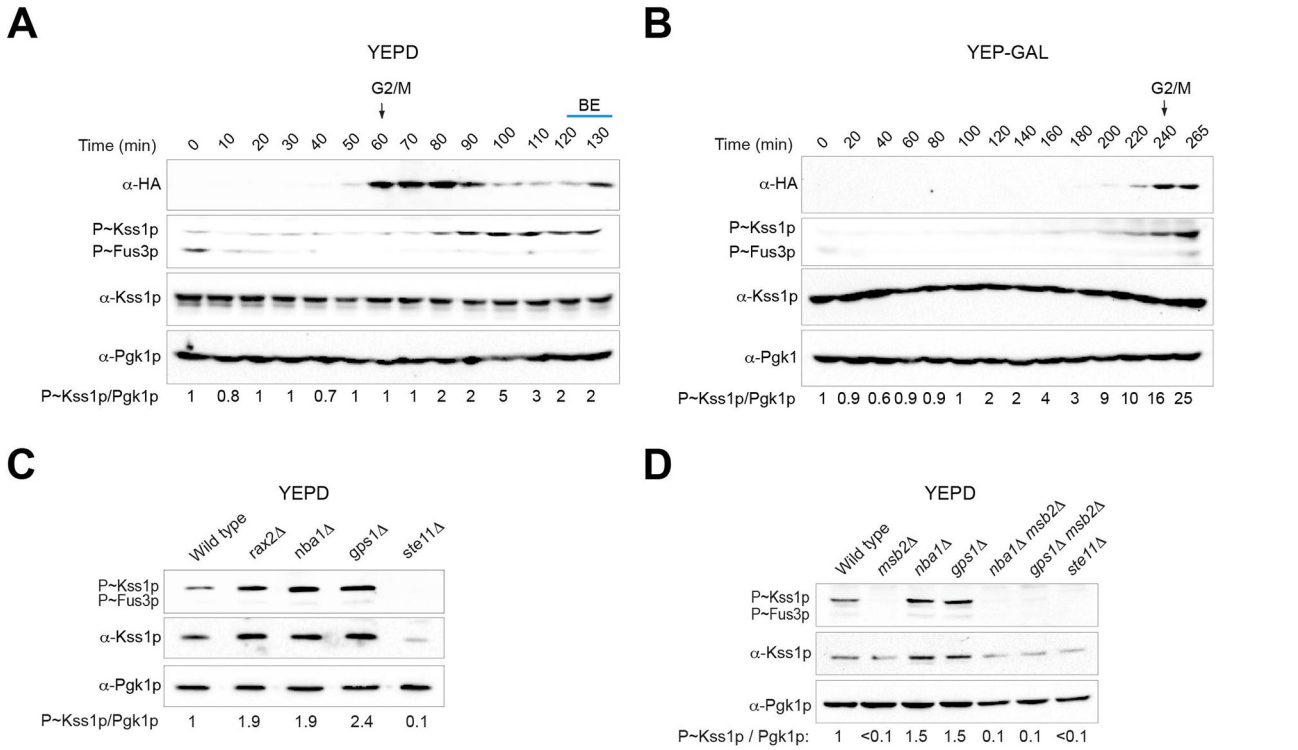

Fig. 3. fMAPK pathway activity in synchronized cells and in mutants that fail to inhibit budding at dormant sites. (A) Immunoblot analysis of wild-type cells synchronized in G_1 by α-factor arrest and released in YEPD. Cell extracts were probed at the indicated time points with antibodies to Clb2p-HA (α-HA), P∼Kss1p (α-p44/42) and Pgk1p as a control for protein levels. Numbers refer to the ratio of P∼Kss1p to Pgk1p relative to 0 min, which was set to 1. BE, bud emergence. (B) Same as panel A, except cells were released into YEP-GAL medium. (C) Immunoblot analysis of wild-type and mutant combinations to assess fMAPK pathway activity. (D) Immunoblot analysis of the role of Msb2p in regulating fMAPK pathway activity in mutants lacking the negative polarity complex. See panel 3A for details.

Journal of Cell Science (2020) 133, jcs241513. doi:10.1242/jcs.241513

activity (Fig. 3C; Fig. S4A), which indicates that the negative polarity complex negatively regulates the fMAPK pathway. The elevated activity of the fMAPK pathway in negative polarity complex mutants also required Msb2p (Fig. 3D; Fig. S4A,B). Cells lacking the negative polarity complex did not have an impact on mating (Fig. S4C). Therefore, proteins that spatially promote budding promote fMAPK activity, and proteins that spatially restrict budding also restrict fMAPK pathway activity. Cells lacking other Cdc42p-interacting proteins, Boi1p and Boi2p (Bender et al., 1996; Glomb et al., 2020; Liao et al., 2013; Masgrau et al., 2017) and Msb1p (Bender and Pringle, 1991; Bi et al., 2000; Liao et al., 2013) were examined but did not show altered activity of fMAPK pathway or a difference in invasive growth compared to wild-type cells (Fig. S4D–I). Collectively, the data indicate that fMAPK pathway activity is temporally and spatially regulated to coincide with bud emergence.

The fMAPK pathway stimulates rate of bud emergence during filamentous growth

To further define how the fMAPK pathway regulates bud emergence, the timing of bud emergence was examined using a septin marker (Cdc3p-mCherry) that shows a characteristic localization pattern throughout the cell cycle (Kim et al., 1991; Lippincott et al., 2001). In yeast-form cells grown in SD-URA (GLU), the timing of GFP-Cdc42p clustering, septin recruitment by Cdc3p-mCherry and bud emergence were similar between wild-type cells and an fMAPK pathway mutant (Fig. S5A). In filamentous wild-type cells grown in S-GAL-URA (GAL), GFP-Cdc42p clustering occurred at the incipient site by 10 min [Fig. 4A (green arrowheads) and 4B (Movie 1)] from the preceding round of cytokinesis marked by the septin hourglass split into a double ring (Fig. 4A; set as t=0; Cid et al., 2001; Lippincott et al., 2001). The recruitment of Cdc3p-mCherry also occurred by 10 min [Fig. 4A (red arrowheads) and 4B (Movie 1)]. The average time for bud emergence for 17 wild-type cells was 30 min from the preceding round of cytokinesis (Fig. 4B). Strikingly, in an fMAPK pathway mutant grown under filamentous conditions (GAL), a delay in GFP-Cdc42p clustering, Cdc3p-mCherry recruitment and bud emergence were observed (Fig. 4B). Although initial GFP-Cdc42p clustering and Cdc3p-mCherry recruitment occurred within the same time span (Fig. 4B,C; example 1, green and red arrowheads), some cells showed disappearance and reappearance of the GFP-Cdc42p cluster at the polarity site [Fig. 4C,D (oscillation seen in the pixel intensity graphs); Movies 2–4]. The disappearance and reappearance of the GFP-Cdc42p cluster, referred to here as transient disappearance of the polarity complex, accounted for a significant delay in bud emergence in the fMAPK pathway mutant (Fig. 4B,C). Some cells failed to make buds within the time of the experiment (Fig. 4D; Movies 3,4). In other examples, the initial polarity site disappeared and reappeared at a new site from where the bud emerged [Fig. 4E (in the mother cell, compare the location of green and red arrowheads with the black arrow that marks bud emergence); Movies 5,6]. The transient disappearance of the polarity complex, seen at some level in wild-type cells (although they always made a bud), was increased by 3-fold in the fMAPK mutant (Fig. 4F). Representing GFP-Cdc42p intensity in each cell as the coefficient of variation (CV) of pixel intensity (Lai et al., 2018) over time brought out the polarity defect in the fMAPK mutant relative to the wild-type (Fig. 4G). The CV of pixel intensity also showed a larger change in wild-type (0.16 to 0.23: 7) compared to the *ste12*Δ mutant (0.14 to 0.18: 4), which was statistically significant (P<0.01). These results define a function for the fMAPK pathway in stimulating the rate of bud emergence under conditions that promote filamentous growth.

To look at active Cdc42p during bud emergence in filamentous conditions, Gic2p-PBD-tdTomato reporter was co-localized with Sho1p-GFP, an fMAPK pathway regulator which is a direct effector of Msb2p (Cullen et al., 2004; Tatebayashi et al., 2007) that interacts with Cdc24p (Vadaie et al., 2008), Ste20p and Ste11p (Tatebayashi et al., 2006; Zarrinpar et al., 2004). Although Sho1p is known to localize to polarized sites (Pitoniak et al., 2009), whether it localizes to presumptive bud sites is not known. In wild-type cells, Sho1p-GFP was localized to incipient bud sites prior to bud emergence together with GTP-Cdc42p (Fig. S5B,C; wild-type, red arrow). After bud emergence, Sho1p-GFP was found at the bud tips as has been reported previously (Pitoniak et al., 2009). In *tec1*Δ mutant cells, Sho1p-GFP initially localized to the incipient bud site but failed to become enriched, and instead migrated back and forth along the distal pole (Fig. S5C; *tec1*Δ, black arrows). The low level of active Cdc42p in these cells rapidly disappeared. Bud formation was delayed and, in the cell shown, bud emergence did not occur within the time of the experiment. Thus, although active Cdc42p clusters at incipient bud sites, an intact fMAPK pathway is required to promote bud emergence under nutrient-limiting conditions. Cells lacking the fMAPK pathway showed a growth defect under filamentous conditions (Fig. S5D; GAL) and a defect in the rate of bud formation (Fig. S5E,F). In particular, at 5, 10 and 18 h, the *ste12*Δ mutant formed buds at a slower rate than wild-type cells. Therefore, the fMAPK pathway stimulates the rate of budding during filamentous growth.

Activation of the fMAPK pathway induces growth at multiple sites

Wild-type cells normally grow at a single site due to a regulatory phenomenon known as singularity in budding. Cells containing active versions of Cdc42p bypass this regulation and grow at multiple sites (Caviston et al., 2002; Howell et al., 2012, 2009; Richman and Johnson, 2000; Wedlich-Soldner et al., 2003, 2004). Cells containing hyperactive versions of Msb2p also had this property (Fig. 5A; Basu et al., 2016). Further inspection showed that 16% of cells carrying $MSB2^{\Delta 100\text{-}818}$ showed multiple growth sites (Fig. 5B; $MSB2^{\Delta 100\text{-}818}$). Given that the fMAPK pathway regulates bud emergence, the ability of Msb2p to induce multiple growth sites might be mediated by the fMAPK pathway. We found that the formation of multiple growth sites by $MSB2^{\Delta 100\text{-}818}$ required the fMAPK pathway (Fig. 5B; $MSB2^{\Delta 100\text{-}818}$ *ste12*Δ). Growth at multiple sites was also induced by *STE11-4* or over-expression of *SHO1* (Fig. 5B). Generally speaking, the formation of multiple growth sites correlated with fMAPK pathway activity (Fig. 5B,C). One exception was *GAL-SHO1*, which showed high levels of multiple growth site formation (Fig. 5B), yet modestly induced fMAPK pathway activity (Fig. 5C). This may be because over-expression of *SHO1* induces a unique cell morphology where cells have hyper-elongated buds (Fig. 5D). The activity of the fMAPK pathway is stimulated by positive feedback, which is evident by immunoblot of the Kss1p protein (Fig. 5C, middle blot), whose levels are controlled by the fMAPK pathway (Roberts et al., 2000). In some fMAPK hyperactive mutants ($MSB2^{\Delta 100\text{-}818}$ and *STE11-4*) the levels of total Kss1p were lower than would be expected by positive feedback. Although the reason for this is not known, it could be due to the presence of negative feedback that acts to attenuate the activated pathway. Thus, Msb2p might itself induce multiple growth sites but require the fMAPK pathway for positive feedback. However, this was not the case. $MSB2^{\Delta 100\text{-}818}$ expressed

Journal of Cell Science (2020) 133, jcs241513. doi:10.1242/jcs.241513

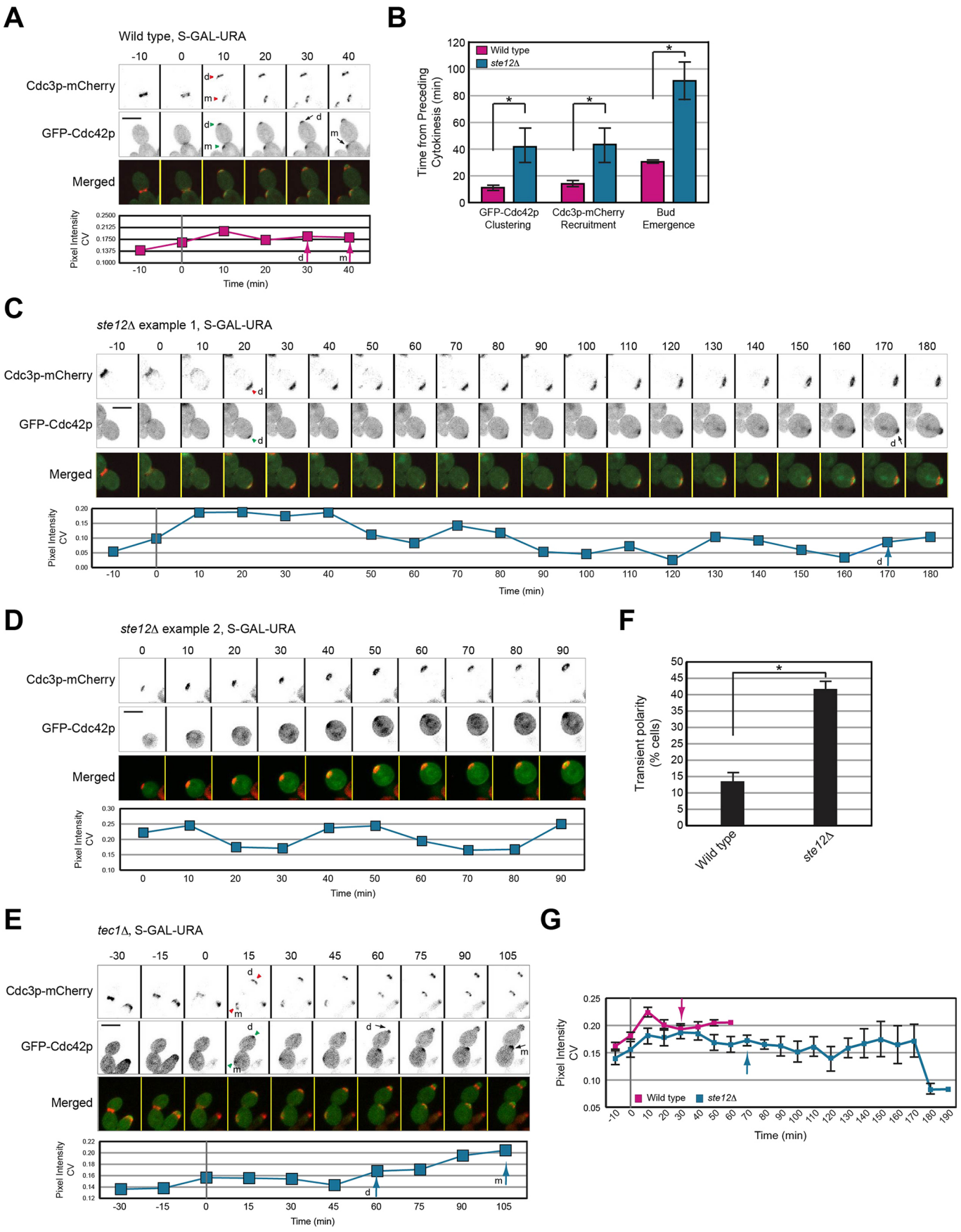

Fig. 4. See next page for legend.

Fig. 4. Role of the fMAPK pathway in regulating bud emergence during filamentous growth. (A) Inverted maximum intensity projection of GFP-Cdc42p clustering and bud emergence in wild-type cells in GAL. Cdc3p-mCherry was used as a marker for cell cycle progression. Septin hourglass split into double ring was set as time 0. Green arrowheads, first visible cluster of GFP-Cdc42p. Red arrowheads, recruitment of Cdc3p-mCherry at incipient sites. Arrows mark bud emergence. Graph represents GFP-Cdc42p intensity over time measured as coefficient of variance (CV) of pixel intensity of the entire cell. Arrow, timing of bud emergence. Scale bar, 5 µm. m, mother cell; d, daughter cell. (B) Quantitation of the timing of GFP-Cdc42p clustering, Cdc3p-mCherry recruitment and bud emergence in wild-type cells and *ste12*Δ cells grown on semi-solid S-GAL-URA medium. Error bars represent s.e.m.; **P*<0.05. (C) Same as in panel 4A, except that the *ste12*Δ mutant was examined. (D) Same as panel 4C, except that *t*=0 represents start of experiment. Time points for the preceding cell cycle were not available for this cell. (E) Same as panel 4A, except that the *tec1*Δ mutant was examined. (F) Cells showing transient disappearance of the polarity complex (expressed as a percentage of the total cells) based on co-localization of GFP-Cdc42p and Cdc3p-mCherry in cells from panel 4B. Error bar represents s.e.m. of 17 cells. **P*<0.01. (G) GFP-Cdc42p intensity over time measured as pixel intensity CV for indicated strains from panel 4B. Error bars represent the s.e.m.

from an inducible promoter (*pGAL*) that did not depend on the fMAPK pathway also required Ste12p to form multiple growth sites (Fig. 5B,C; compare *GAL-MSB2*$^{\Delta100\text{-}818}$ with *GAL-MSB2*$^{\Delta100\text{-}818}$ *ste12*Δ). Therefore, Msb2p activation itself is not sufficient to induce growth at multiple sites. The fact that *MSB2*$^{\Delta100\text{-}818}$ is more effective at inducing growth at multiple sites than *STE11-4* can be explained by fMAPK pathway activity.

Transcriptional targets of the fMAPK pathway may be required for the formation of multiple growth sites. Bni1p and Gic2p were required for multiple growth site formation by the fMAPK pathway (Fig. 5E). High-copy expression of *GIC2* itself induced multiple growth sites (Fig. 5E), in line with a previous report (Jaquenoud et al., 1998). The negative polarity complex did not have an impact on growth at multiple sites (Fig. 5B; p*STE11-4 nba1*Δ), although it did stimulate the fMAPK pathway activity (Fig. 5C). Collectively, these results support a role for the fMAPK pathway in the regulation of bud emergence, because activation of the fMAPK pathway can induce growth at multiple sites.

The fMAPK pathway induces symmetry breaking in the growing bud

The multiple growth sites produced by the fMAPK pathway differed in shape from previous reports on multiple bud formation by hyperactivation of Cdc42p (Caviston et al., 2002; Wedlich-Soldner et al., 2003, 2004). Hyperactive Cdc42p induces symmetry breaking in the mother cell to trigger formation of a second bud. By comparison, the hyperactive fMAPK pathway did not affect budding in mother cells. The multiple growth sites were formed inside the growing bud (Fig. 6A). To our knowledge, this new phenotype has not been previously characterized. Growth at a second site within the growing bud was not due to abortive growth at the initial site, because polarity proteins including Cdc24p-GFP (Fig. 5D) localized to multiple sites. Actin dynamics in live cells using Abp140p-YFP, a marker for the actin cables (Asakura et al., 1998; Riedl et al., 2008; Yang and Pon, 2002), showed multiple growth sites in the hyperactive fMAPK mutants compared with wild-type cells (Fig. 6B). Actin staining in filamentous cells using rhodamine phalloidin also showed polarized actin cytoskeleton at more than one site (Fig. S6A–C). Cells expressing *MSB2*$^{\Delta100\text{-}818}$ showed asymmetric clustering of GFP-Cdc42p (Fig. 6C; Movie 8). Over time, GFP-Cdc42p migrated along the bud cortex (Fig. 6C), which was evident by kymograph analysis (Fig. 6D), which allows tracking of changes in protein localization over time (Kaksonen et al., 2003). Sec3p-GFP localization corroborated that these sites were actively growing (Fig. S6C). Some wandering of GFP-Cdc42p occurred in wild-type cells (Movie 7), which might be due to the off-center delivery of vesicles that dilute the polarity complex (Chiou et al., 2017; Dyer et al., 2013).

The hyperactive fMAPK pathway may alter the dynamics of the interaction between Cdc42p and its effectors in a manner that makes the Cdc42p polarity axis 'forget' its orientation. This may mimic symmetry breaking occurring but within the bud cortex. In line with this possibility, versions of Cdc42p that contain point mutations in the effector-binding domain (such as Cdc42p^{V36T}), which impair its interaction with effector proteins (Gladfelter et al., 2002, 2005, 2001), showed a similar phenotype (Fig. 6E). Here multiple protrusions occurred adjacent to the previous polarization site. Similarly, cells expressing *MSB2*$^{\Delta100\text{-}818}$ formed multiple growth projections (Fig. 6A; three, four or five sites). Other genes can induce multiple buds when over-expressed (Sopko et al., 2006), but these did not rescue the growth defect of the *cdc24-4* mutant and in most cases made it worse (Fig. S6D). These results demonstrate the importance of a properly regulated fMAPK pathway in bud morphogenesis.

DISCUSSION

Here we show that bud emergence, which is one of the most intensively studied and well understood polarity establishment processes in eukaryotes, is regulated by a MAPK pathway. The fMAPK pathway regulates transcription of polarity target genes and GTP-Cdc42p levels to increase the rate of bud emergence during filamentous growth. In this way, bud emergence is regulated by a pathway whose activity is sensitive to extrinsic cues. Importantly, the ability of the fMAPK pathway to induce the expression of polarity target genes allows the pathway to tailor bud emergence by altering the levels of proteins that act at multiple steps in the polarity pathway.

The fMAPK pathway may also regulate bud emergence during vegetative growth. Ste20p is the first effector recruited by Cdc42p at bud sites (Moran et al., 2019), which is known to activate the fMAPK pathway at bud sites to regulate bud emergence. Ste12p and Tec1p are also required for viability of the *cdc24-4* mutant under vegetative growth conditions. A function for the fMAPK pathway in regulating bud emergence might be masked by genetic buffering under normal growth conditions. Indeed, cells lacking *TEC1* are synthetically lethal with a diverse class of cytoskeletal and cell-cycle regulatory genes (Costanzo et al., 2010). More recently, Rsr1p in its GDP-locked state has been shown to regulate the timing of Cdc42p polarization in early G_1 by interaction with Bem1p (Miller et al., 2019). Rsr1p (Basu et al., 2016) and Bem1p (Basu et al., 2020) both regulate the fMAPK pathway.

A key polarity target of the fMAPK pathway is Gic2p, which is a direct effector of Cdc42p that controls multiple steps in bud emergence. The regulation of *GIC2* expression may be a key step in regulating polarity establishment in general. *GIC2* expression is regulated by the fMAPK pathway and other proteins that regulate filamentous growth, including Phd1p (Gimeno and Fink, 1994; MacIsaac et al., 2006), Rim101p (Hu et al., 2007; Lamb and Mitchell, 2003), SAGA (Venters et al., 2011) and Rpd3p(L) (Hu et al., 2007; Venters et al., 2011). *GIC2* expression is also regulated during mating (Roberts et al., 2000) and the Gic proteins are required for shmoo formation (Brown et al., 1997). Gic2p may function in other contexts as well, and has been implicated as an effector of the protein kinase C pathway (Zanelli and Valentini, 2005). Generally speaking, changes in gene expression may affect the

Journal of Cell Science (2020) 133, jcs241513. doi:10.1242/jcs.241513

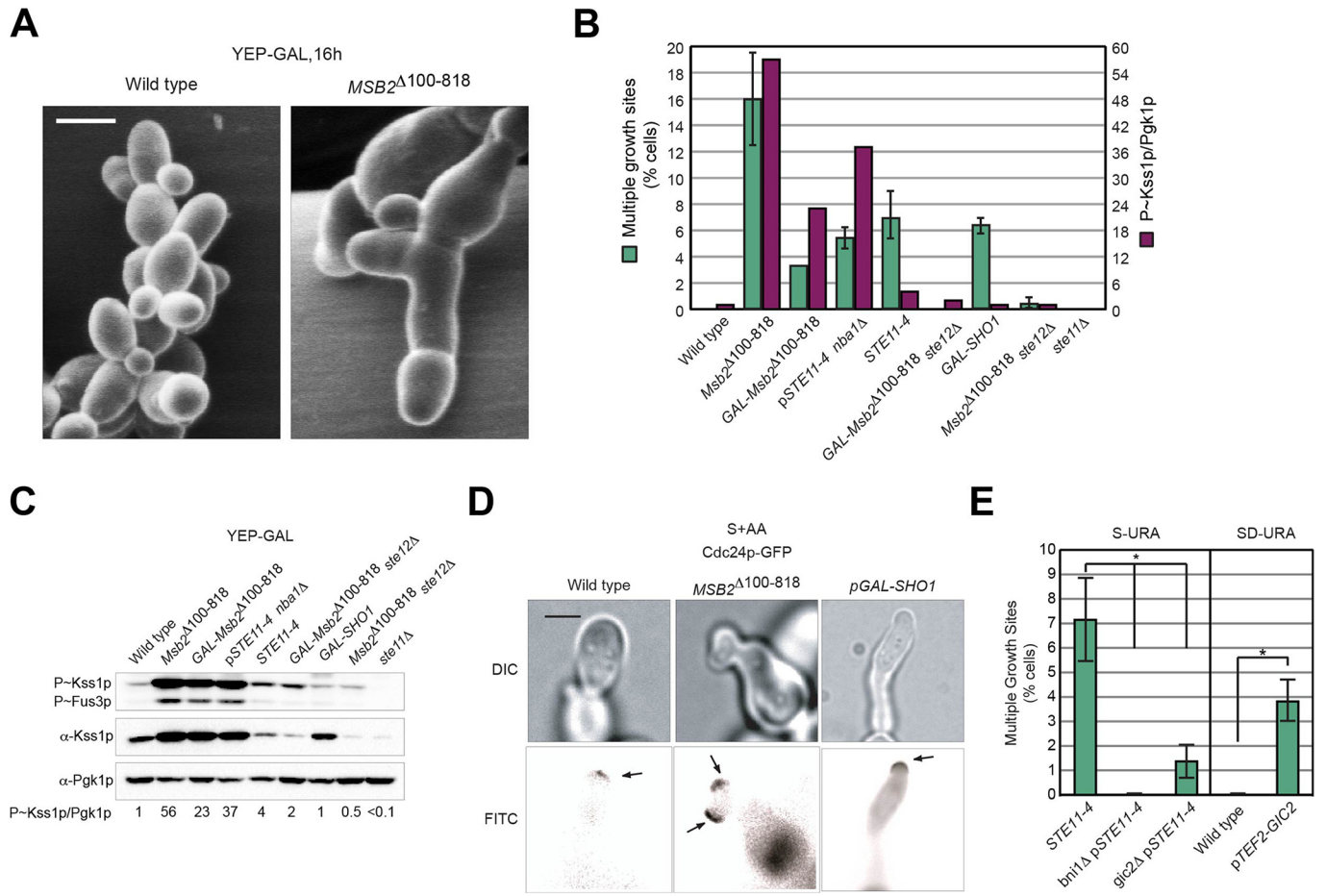

Fig. 5. Hyperactivation of the fMAPK pathway induces multiple growth sites. (A) Scanning electron micrographs of wild-type and *MSB2*$^{\Delta 100\text{-}818}$ examined for multiple growth sites. Scale bar, 5 µm. (B) Comparison of percentage of multiple growth sites by the single cell assay with P~Kss1p levels in panel C in the indicated strains (*n*>50 cells). Error bars represent s.e.m. from three separate trials. The histogram for P~Kss1p represents the ratio of P~Kss1p to Pgk1p relative to wild-type, which was set to 1. (C) Immunoblot analysis of fMAPK activity in the indicated strains grown in YEP-GAL. Pgk1p, loading control. Numbers refer to the ratio of P~Kss1p to Pgk1p relative to wild-type, which was set to 1. (D) Wild-type cells and cells harboring the *MSB2*$^{\Delta 100\text{-}818}$ and *GAL-SHO1* alleles containing Cdc24p-GFP were examined by the single cell invasive growth assay. No glucose was added to S+AA medium. Arrows point to Cdc24p-GFP at the growing tip. Scale bar, 5 µm. (E) Percentage of multiple buds by the single cell assay in indicated strains. In a separate experiment, wild-type cells expressing *TEF2-GIC2* were grown to saturation and evaluated for the percentage of multiple buds. See panel B for details. **P*<0.01.

regulation of bud emergence during cell differentiation and the response to stress.

Here and in Basu et al. (2016), we identify cross-talk between the polarity pathway and the fMAPK pathway. Cross-talk from the fMAPK pathway to the polarity pathway impacts bud emergence in several ways: (1) the activity of the fMAPK pathway is amplified by positive feedback to stimulate GTP-Cdc42p levels, (2) the fMAPK pathway induces target genes that encode polarity pathway components, and (3) the fMAPK pathway induces target genes that prevent growth at dormant growth sites (Meitinger et al., 2013). We also show that the activity of the fMAPK pathway is critical for proper bud emergence. Too little fMAPK pathway activity causes a delay in bud emergence during filamentous growth, and too much leads to growth at multiple sites. Precise regulation of the fMAPK pathway comes from activation at the right place (incipient bud sites) and time (at M/G_1). The fact that the fMAPK pathway is cell-cycle regulated is a novel finding. Cell-cycle regulation of the fMAPK pathway might occur through *TEC1*, which like other G_1 specific genes in the 'SIC' cluster (Cho et al., 1998; Spellman et al., 1998; Wittenberg and Reed, 2005) is induced at the M/G_1 boundary by the cell-cycle regulated transcription factor Swi5p (Spellman et al., 1998).

During vegetative growth in *S. cerevisiae*, Cdc42p-dependent budding is dictated by bud-site-selection proteins (Chiou et al., 2017). In other fungal species, diverse mechanisms of polarity control predominate. In *Schizosaccharomyces pombe*, growth at the two poles is maintained by regulated oscillations in Cdc42p activity (Das et al., 2012). Changes in the orientation of the polarity complex occur during mating (Dyer et al., 2013; Nern and Arkowitz, 2000) and filamentous growth (this study), and may be a common feature of fungal cell differentiation. In the filamentous fungus *Ashbya gossypii*, Rsr1p regulates symmetric growth cone formation at the hyphal tip (Bauer et al., 2004). In the major human fungal pathogen *Candida albicans*, Rsr1p and Cdc42p are also required for proper hyphal growth (Si et al., 2016). MAPK pathways may be critical regulators of Cdc42p-dependent morphogenesis during hyphal/pseudohyphal growth. Parallels can also be drawn to higher eukaryotes. In mammals, the ERK pathway is directly involved in breaking radial symmetry of spreading RAT2 fibroblast cells (Klímová et al., 2016). In this case, ERK spatially restricts p190A-RhoGAP activity to limit growth at the cell rear. Functional cross-talk between MAPK pathways and Rho GTPases may constitute an under-explored regulatory circuit in many systems.

Journal of Cell Science (2020) 133, jcs241513. doi:10.1242/jcs.241513

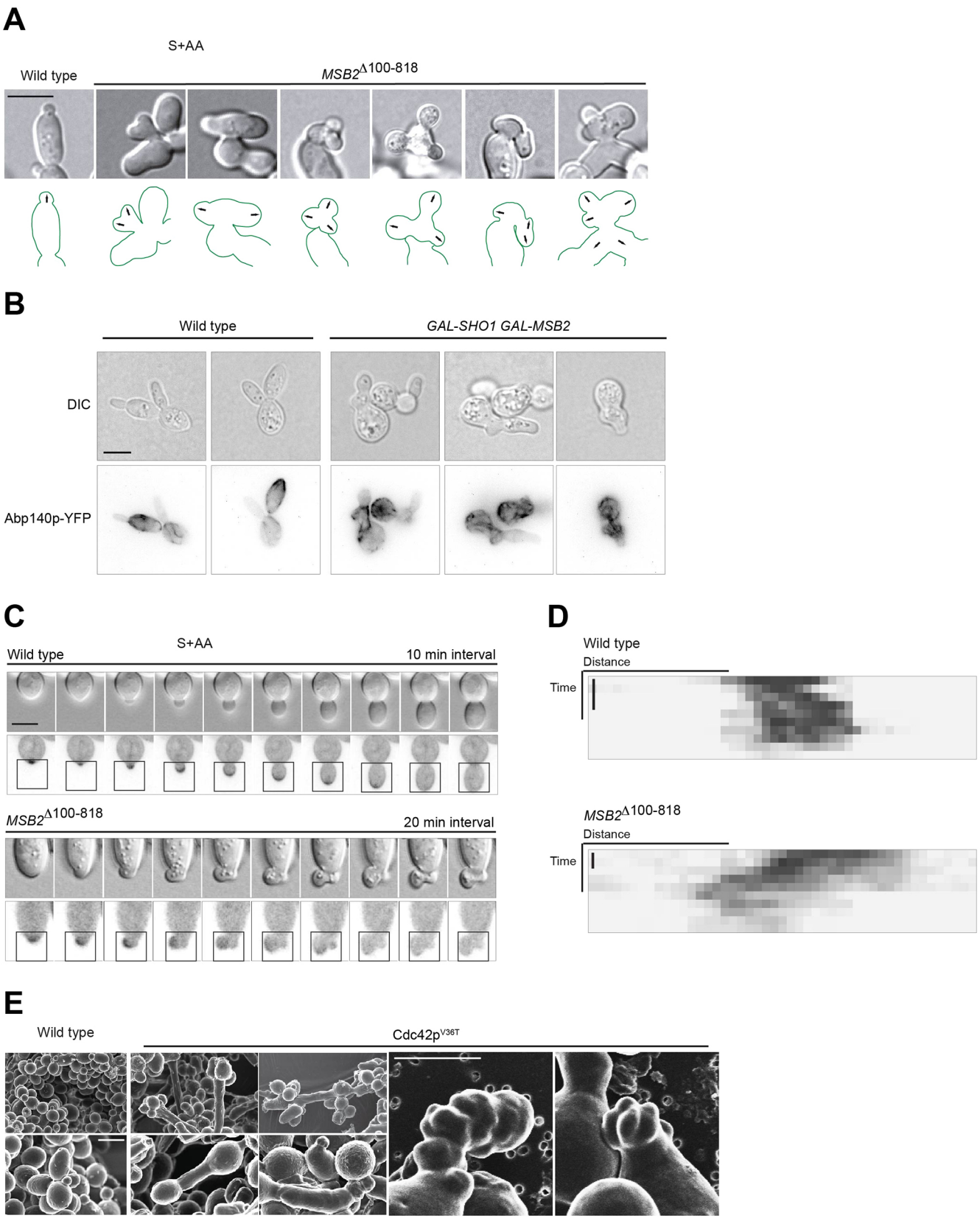

Fig. 6. Activation of the fMAPK pathway leads to wandering polarity. (A) Wild-type cells and cells carrying *MSB2*$^{\Delta 100\text{-}818}$ were examined on S-GLU medium by the single cell invasive growth assay. Arrows indicate growth sites. Scale bar, 5 µm. (B) Wild-type and cells containing *GAL-SHO1* and *GAL-MSB2* harboring Abp140p-YFP, a marker for the actin cytoskeleton, were examined for actin cable dynamics in S-GAL+AA semi-solid agar medium. Scale bar, 5 µm. (C) Time series of growth of wild-type cells and cells harboring *MSB2*$^{\Delta 100\text{-}818}$ expressing GFP-Cdc42p evaluated for multiple growth sites. Scale bar, 5 µm. Time interval: WT, 10 min; *MSB2*$^{\Delta 100\text{-}818}$, 20 min. DIC and inverted maximum intensity projection are shown. (D) Kymograph analysis of the highlighted regions in panel C. Time scale bar, 40 min. (E) Scanning electron micrographs of wild-type and Cdc42p^{V36T}. Scale bar, 5 µm.

Journal of Cell Science (2020) 133, jcs241513. doi:10.1242/jcs.241513

MATERIALS AND METHODS

Strains and plasmids

Yeast strains are described in Table S1. Plasmids are listed in Table S2. Gene disruptions and *GAL1* promoter fusions were made by polymerase chain reaction (PCR)-based methods (Baudin et al., 1993; Longtine et al., 1998). Some gene disruptions were made with antibiotic resistance markers *KanMX6* (Longtine et al., 1998), *HYG* and *NAT* (Goldstein and McCusker, 1999). Internal epitope fusions were made by the pop-in, pop-out strategy (Schneider et al., 1995). Some strains were made *ura3-* by selection on 5-fluoroorotic acid (5-FOA). Gene disruptions were confirmed by PCR Southern analysis and confirmed by phenotype when applicable.

The pRS series of plasmids (pRS315 and pRS316) have been described (Sikorski and Hieter, 1989). To construct *cdc24-4* mutant (PC6936), NAT cassette in PC6077 was replaced with *URA3* using pop-in, pop-out strategy (Schneider et al., 1995). Following complementary primers were used: 5′-CAGAAGAGTACCATTGCTGTTATCATTTGTTGCCTAGCCCTATCA-ACTAAAGGGAACAAAAGCTGG-3′ and 5′-CAATATAATGGGTATA-GCTTGAACATCTGCCCCTCTCTATCTAATGTCACTATAGGGCGAA-TTGG-3′. The strain was subsequently made *ura3*Δ by selection on 5-FOA. *cdc24*Δ was confirmed by phenotypic analysis. Msb2p (p*GFP-MSB2*; Adhikari et al., 2015), Sho1p (pRS316-*SHO1*^{D16H,P120L}*-GFP* or *SHO1*^{P120L}; Vadaie et al., 2008) and Ste11p (YCp50-*STE11-4*; Stevenson et al., 1992) have been described. Plasmid pRS316-*SHO1-GFP* has been described (Marles et al., 2004) and was provided by Dr Alan Davidson (University of Toronto, Ontario, Canada). In *SHO1*^{D16H}, the D16H mutation alone does not hyperactivate the fMAPK pathway, but together with P120L mutation results in a hyperactive version of the protein. Over-expression constructs came from an ordered collection (Gelperin et al., 2005). YEp352-*TEF2-GIC2* was created by amplifying the *GIC2* open reading frame (ORF) by PCR from genomic DNA using complementary primer pairs 5′-GACTCTAGAATGACTAGTGCAAGTATTACCAATACTGGA-AACG-3′ and 5′-CAGTGTCGACTTAAGTTTGCAGGGGCTCGAGC-3′. The PCR product was digested with XbaI and SalI and inserted into the YEp352-*TEF2* plasmid (Pitoniak et al., 2015) digested with the same enzymes. Positive clones were confirmed by DNA sequencing.

Plasmid YCplac181-*CDC12-GFP::KanMX6* was constructed from YCplac181-*CDC12-GFP* (PC1365), provided by John Pringle (Stanford University) (Fares et al., 1996), by homologous recombination. The *KanMX6* cassette was amplified by PCR with flanking sequences to *LEU2* locus on the YCplac181-*CDC12-GFP* plasmid. Complementary primers were designed: 5′-ATGTCTGCCCCTAAGAAGATCGTCGTTTTGCCA-GGTGACCACGTTGCGGATCCCCGGGTTAATTA-3′ and 5′-TTAAG-CAAGGATTTTCTTAACTTCTTCGGCGACAGCATCACCGACTGAAT-TCGAGCTCGTTTAAAC-3′ (Millipore Sigma, St Louis, MO, USA). The PCR product was co-transformed with YCplac181-*CDC12-GFP* digested with AflII to target integration at the *LEU2* locus. Plasmids were rescued from isolates that were *KanMX6* positive. YCplac181-*CDC12-GFP::NAT* was made by the same strategy.

pRS316-*GFP-CDC42::KanMX6* was made from pRS316-*GFP-CDC42* (PC6454) by targeting integration at the *URA3* locus using complementary primers 5′-ATGTCGAAAGCTACATATAAGGAACGTGCTGCTACTC-ATCCTAGTCGGATCCCCGGGTTAATTA-3′ and 5′-TTAGTTTTGCT-GGCCGCATCTTCTCAAATATGCTTCCCAGCCTGGAATTCGAGCT-CGTTTAAAC-3′ (Millipore Sigma). pRS316-p*ACT1-EGFP*-CRIB*CLA4-CDC42*$^{\Delta CAAX}$-mCherry-CAAX*::KanMX6* was made from pRS316-p*AC-T1-EGFP*-CRIB*CLA4-CDC42*$^{\Delta CAAX}$-mCherry-CAAX (PC7137) (Smith et al., 2013) and p*SHO1*^{D16H}*-GFP::KanMX6* was made from p*SHO1*^{D16H}*-GFP* (PC1964) by targeting integration at the *URA3* locus using the same complementary primers as for pRS316-*GFP-CDC42::Ka-nMX6*. The PCR product was co-transformed with plasmids digested with BsmI to target integration at the *URA3* locus. Plasmids were rescued from isolates that were *KanMX6* positive. pRS316-*GFP-CDC42::NAT* and p*S-HO1*^{D16H}*-GFP::NAT* were made by the same strategy.

Plasmids were recovered from cells with Promega Wizard Plus SV Miniprep DNA Purification system (A1460, Promega, Madison, WI, USA) used as specified by the manufacturer with the following modifications: 100 µl of glass beads were added at the lysis step, and cells were vortexed for 5 min before the addition of neutralization buffer. Rescued plasmids were transformed into *Escherichia coli*, and positive clones were confirmed by DNA sequencing, by GENEWIZ (South Plainfield, NJ, USA) and by fluorescence microscopy after transformation in yeast.

Filamentous growth and mating assays

Yeast and bacterial strains were manipulated by standard methods (Rose et al., 1990; Sambrook et al., 1989). The single-cell invasive growth assay (Cullen and Sprague, 2000) and the plate-washing assay (Roberts and Fink, 1994) were performed as described. Actin staining by rhodamine phalloidin was performed as described (Yuzyuk and Amberg, 2003). In cells lacking an intact mating pathway (*ste4*Δ), the *FUS1-HIS3* reporter (McCaffrey et al., 1987) was used to evaluate fMAPK pathway activity (Cullen et al., 2004). *FUS1-HIS3* activity was measured by spotting equal concentrations of cells onto SD-HIS medium and SD-HIS medium containing 3-amino-1,2,4-triazole (3-ATA).

Halo assays were performed as described (Jenness et al., 1987). A saturated culture of cells (A_{600}=0.1) was spread on YEPD medium and allowed to dry. α-Factor (3 µl and 10 µl, at 1 mg/ml) was spotted on the plates. Plates were incubated at 30°C and photographed at 24 and 48 h. Experiments were performed in triplicate. Halo diameter (in centimeters) was measured by ImageJ analysis and plotted as a function of α-factor concentration. For Lat-A sensitivity, saturated culture of cells (A_{600}=0.1) was spread onto SD-URA-LEU medium containing 0.5 M sorbitol. Lat-A (10 µl; L5163, Sigma) at 0, 0.1, 0.2 and 0.5 mM (in 10 mM DMSO) were spotted on plates. Halo diameter (in centimeters) was measured by ImageJ analysis and plotted as a function of Lat-A concentration.

Evaluating MAP kinase phosphorylation by immunoblot analysis

Immunoblot analysis was used to detect phosphorylated MAP kinases as described (Basu et al., 2016; Lee and Dohlman, 2008; Sabbagh et al., 2001). In *cdc24-4* mutant combinations, cells were grown to mid-log in 10 ml SD-URA at 30°C and then incubated at 37°C for 4 h. Cells were harvested by centrifugation. Pellets were washed once with water and flash-frozen in liquid nitrogen. In experiments that did not involve *cdc24-4*, cells were grown in YEPD or YEP-GAL media for the times indicated. Proteins were precipitated by trichloroacetic acid (TCA) and analyzed by sodium dodecyl sulfate polyacrylamide gel electrophoresis (SDS-PAGE) (10% acrylamide). Proteins were transferred to nitrocellulose membranes (Amersham Protran Premium 0.45 µm NC; 10600003, GE Healthcare Life Sciences).

Cell synchronization and cell cycle analysis of MAPK activity

Cell synchronization experiments were performed as described (Breeden, 1997). The strain harboring Clb2p-HA (PC2744) was transformed with a plasmid containing the *STE4* gene (p*STE4*; Stevenson et al., 1992). Cells were grown to an optical density (OD) A_{600} of 0.2 in SD-URA medium. Cells were washed and resuspended in equal volume of YEPD and incubated for 90 min at 30°C. α-Factor was added to a final concentration of 5 µg/ml and the culture was incubated for 90 min to arrest cells in the G_1 phase of the cell cycle. Arrested cells were washed twice with water and resuspended in fresh YEPD or YEP-GAL medium to release cells into the cell cycle. Aliquots (10 ml) were harvested every 10 min, flash-frozen in liquid nitrogen and stored at −80°C.

Immunoblot analysis

ERK-type MAP kinases (P∼Kss1p and P∼Fus3p) were detected using p44/42 antibodies (no. 4370; Cell Signaling Technology, Danvers, MA, USA) at a 1:5000 dilution. Kss1p was detected using α-Kss1p antibodies (no. 6775; Santa Cruz Biotechnology, Santa Cruz, CA, USA) at a 1:5000 dilution. Clb2p-HA was detected using the α-HA antibody at a 1:5000 dilution (no. 12CA5; Roche Diagnostics). For secondary antibodies, goat anti-rabbit IgG-HRP antibodies were used at a 1:10,000 dilution (no. 111-035-144; Jackson ImmunoResearch Laboratories, West Grove, PA, USA). Mouse α-Pgk1p antibodies were used at a 1:5000 dilution as a control for total protein levels (no. 459250; Thermo Fisher Scientific, Waltham, MA, USA). Goat α-mouse secondary antibodies were used at a 1:5000 dilution to detect primary antibodies (no. 170-6516; Bio-Rad Laboratories, Hercules, CA, USA). Blots were visualized by chemiluminescence using a Bio-Rad ChemiDoc XRS+ system (1708265, Bio-Rad). Quantitation of band intensities for immunoblot

analysis was performed with Image Lab Software (Bio-Rad). For blots to evaluate phosphorylated MAP kinase proteins, membranes were incubated in 1×TBST (10 mM TRIS–HCl, pH 8, 150 mM NaCl, 0.05% Tween-20) with 5% bovine serum albumin. For other immunoblots, membranes were incubated in 1×TBST with 5% non-fat dried milk. All primary incubations were carried out for 16 h at 4°C. Secondary incubations were carried out at 25°C for 1 h.

Growth assays for temperature-sensitive mutants

Wild-type and temperature-sensitive mutants containing desired plasmids were grown to saturation in SD-URA media. For each strain, 0.1 OD_{600} of cells were serially diluted four times in distilled water and spotted onto SD-URA-LEU+ 0.5 M sorbitol plates. The plates were incubated at 30 and 37°C. For *cdc12-6* suppression, cells were spotted onto SD-URA plates and incubated at 24 and 30°C as the *cdc12-6* mutant had a severe growth defect at 30°C and failed to grow completely at 37°C. For all suppression assays, plates were photographed every day for 4 days using an Evolution MP Color Camera (Media Cybernetics) and Q Capture software. Images were imported into ImageJ software. Cells of interest were selected and the *measure* tool was used to generate values for the integrated density, area and the mean signal intensity. Growth of a colony was quantified by measuring the signal intensity of the colony against the background using the formula: corrected signal intensity=integrated density−(area of selected cell×mean signal intensity of the background cell). Growth at 37°C was compared with growth at 30°C for each strain and then normalized to wild-type. Quantitation was reported for the day where the temperature-sensitive mutant containing *STE11-4* plasmid showed around 60% of growth compared with the wild-type, which was the maximum growth detected across various mutant combinations and independent trials. For most analyses, only the first or the second dilution of cells was used for the quantitation. All growth assays were performed in triplicate. Error bars show standard error of mean (s.e.m.) among the three trials.

Quantitative PCR analysis

Cells for qPCR were concentrated (OD A_{600}=20) and spotted in 10 µl aliquots onto YEP-GAL (2% agar) for 24 h. Cells were spotted in six colonies per plate equidistant to each other and the plate center. All six colonies were harvested for each trial, and two separate trials were compared for each strain. The entire colony surface was scraped into 500 µl of distilled water, harvested by centrifugation, washed and stored at −80°C. RNA was harvested by hot acid phenol chloroform extraction as described previously (Adhikari and Cullen, 2014). Samples were further purified using Qiagen RNeasy Mini Kit (catalog no. 74104). RNA concentration and purity were measured using NanoDrop (NanoDrop 2000C). RNA stability was determined by 1% agarose Tris-borate-EDTA (TBE, 89 mM Tris base, 89 mM boric acid, 2 mM EDTA) gel electrophoresis.

cDNA libraries from RNA samples were generated using iScript Reverse Transcriptase Supermix (no. 1708840; Bio-Rad). qPCR was performed using iTaq Universal SYBR Green Supermix (no. 1725120; Bio-Rad) on a Bio-Rad CFX384 Real-Time System. Fold changes in expression were determined by calculating ΔΔCt using *ACT1* mRNA as the housekeeping gene for each sample. Experiments were performed with biological replicates, and the average of multiple independent experiments was recorded. Primers for pPCR for *GIC2* were: forward 5′-GCGCCAACAAGACAAATCACAAA-3′ and reverse 5′-GCAATTGCTCATCTTGGAATCC-3′. Primers for *GIC1* were: forward 5′-GCCGAACAAGAACAACATCAA-3′ and reverse 5′-GTTTT-GGCAGACCCATGTCTC-3′. Primers for *ACT1* were: forward 5′-GGCTT-CTTTGACTACCTTCCAACA-3′ and reverse 5′-GATGGACCACTTTCGT-CGTATTC-3′ as published (Chavel et al., 2010).

DIC and fluorescence microscopy

Differential interference contrast (DIC) and fluorescence microscopy using FITC, Cyan Fluorescent Protein (CFP), Yellow Fluorescent Protein (YFP), rhodamine and DAPI filter sets were performed using an Axioplan 2 fluorescent microscope (Zeiss) with a Plan-Apochromat 100×/1.4 (oil) objective (NA 1.4) (cover slip 0.17) (Zeiss). Digital images were obtained with the Axiocam MRm camera (Zeiss) and Axiovision 4.4 software (Zeiss). Adjustments to brightness and contrast were made in Adobe Photoshop. Some images were obtained using structural deconvolution with a Zeiss Apotome filter. Multiple polarization events were assigned by examining cells over multiple focal planes by DIC and fluorescence microscopy. Time-lapse microscopy was performed on a Zeiss 710 confocal microscope equipped with a Plan-Apochromat 40×/1.4 oil DIC M27 objective on a heated stage at 37°C. GFP was imaged using 488 nm laser excitation and an emission window from 496 to 572 nm. Time-lapse *Z*-stacks were captured at 10 and 20 min intervals to monitor bud emergence and Cdc42p clustering.

Budding rate assay

Cells were grown for 16 h on SD+AA medium. Using a toothpick, cells were removed from the plate, washed twice with water and resuspended in 1 ml water. Cells (50 µl) were spread onto SD+AA or S-GAL+AA media and incubated at 30°C. Cells were visualized at 0, 5, 10 and 18 h intervals at 20×. Budding rate, $\ln(n)/\ln(2)$, was determined as described (Hall et al., 2014), where n is the number of daughters produced. Budding rate was adjusted for the time interval (5, 5 and 8 h). More than 30 cells were examined for each interval.

Time-lapse microscopy

For time-lapse microscopy, cells were placed onto semi-solid agarose pads that were prepared as described (Skinner et al., 2013) with the following modifications. Approximately 700 µl of SD-URA medium, prepared with agarose (1%), was placed inside 12 mm Nunc glass base dishes (no. 150680; Thermo Fisher Scientific, Waltham, MA, USA) and allowed to set at 25°C for 5 min.

For GFP-Cdc42p clustering in *cdc24-4* mutant combinations, cells were taken from colonies grown at 30°C for 16 h on SD-URA+G418 semi-sold agar media [2% agarose, 0.67% yeast nitrogen base (YNB) without ammonium sulfate, 0.1% monosodium glutamate (MSG), 2% dextrose, 1× amino acid stock without uracil, 0.36 mg/ml G418], resuspended in 7 µl of synthetic broth (0.67% YNB without ammonium sulfate, 0.1% MSG, 2% dextrose), and placed under the agarose pads by gently lifting the pad with a scalpel. Water (100 µl) was placed in the dish adjacent to the agarose pad to prevent moisture loss, and the Petri dishes were incubated at 37°C for 4 h. For co-localization of Sho1p-GFP and Gic2p-PBD-tdTomato, cells were prepared as above except that they were imaged at 30°C. For GFP-Cdc42p clustering in cells carrying $MSB2^{\Delta 100\text{-}818}$, 500 µl of saturated culture was washed twice with water and resuspended in 500 µl water. An aliquot of 5 µl was placed under the agarose pad, and the Petri dish was incubated at 30°C for 10 h before imaging. For strains expressing GFP-Cdc42p and Cdc3p-mCherry, cells were prepared from colonies grown at 30°C for 16 h on SD-URA.

FLIM-FRET analysis

Plasmids containing the Cdc42p biosensor have been described (Smith et al., 2013) and were a generous gift from Dr Rong Li (Johns Hopkins University, Baltimore, MD, USA). Cells containing pRS316-pACT1-eGFP-CRIBCLA4-$Cdc42p^{\Delta CAAX}$–mCherry-CAAX (PC7137) and Q61L (PC7138) or D57Y (PC7139) derivatives were grown on SD-URA medium to maintain selection for the plasmids. Semi-solid agarose pads were prepared as described above. Cells were taken from colonies grown for 16 h on semi-solid agar medium (SD-URA), resuspended in 7 µl of SD broth, and placed under the agarose pads.

Confocal microscopy and FLIM was performed at the SUNY-Buffalo North Campus Confocal Imaging Facility. FLIM-FRET has been described (Bassard and Halkier, 2018; Gratton et al., 2003; Osterlund et al., 2015; Padilla-Parra et al., 2015; Periasamy and Clegg, 2009; Sun and Periasamy, 2015). FLIM-FRET images were acquired with a Simple Tau TCSPC 150 and HPM-100-40 GaAsP detector (Becker & Hickl, Berlin, Germany) employing the direct coupled port of the LSM 710 and Zeiss Intune Laser excitation at 490 nm. At least 1000 photons per pixel were acquired for the highest count region for each cell.

FLIM-FRET data analysis was performed using SPCImage 7.3 (Becker & Hickl). Data were fitted by a two-component exponential decay model and automatically generated instrument response function (IRF). Bin factor, shift and offset were adjusted to obtain good fit (low χ^2). For measuring the

average lifetime, the decay curve was pooled for the region of interest. The mean fluorescence lifetime for the two-component decay model was calculated according to the equation: $\tau_m=a_1\tau_1+a_2\tau_2$, where a_i and τ_i are the amplitude and lifetime of the ith component and τ_m is the average lifetime of the donor fluorescence.

Scanning electron microscopy

Scanning electron microscopy was based on established methods (Piccirillo and Honigberg, 2011) and performed as described (Basu et al., 2016). For some experiments, cells were grown for 16 h in liquid medium at 30°C. Cells were washed in 0.1 M sodium phosphate buffer at pH 7.4 and diluted to about 10^6 cells, which were passed over 0.2 µm Whatman nucleopore polycarbonate filter paper (catalog no. 889-78084GE Whatman) with a 10 ml syringe (no. 309604 BD Syringe). Cells were rinsed with one round of buffer by syringe, fixed with 1% glutaraldehyde for 15 min, and rinsed again. Cells were treated by a graded series of ethanol washes (30, 50, 70, 85 and 100%) by syringe to dehydrate the samples. The filter paper was removed from the holder, placed in a Petri dish and treated with hydroxymethyldiazane (HMDS). Samples were placed at 4°C for 16 h and imaged the following day. All solutions were filter sterilized before use and stored in clean containers free of corrosion products. Samples were carbon coated and imaged on a field emission scanning electron microscope (Hitachi SU70).

Image analysis

Gic2p-PBD-tdTomato clustering was quantified as described in Okada et al. (2017) with the following modifications. Raw fluorescence and DIC images were imported in ImageJ. DIC images were used to draw the cell boundary with the polygon tool. The same region of interest (ROI) was applied to the fluorescence image. Signal intensities for all pixels inside the ROI were exported as a CSV file using *save XY coordinates* option under the *Analyze tool* menu. A custom MATLAB (MATLAB R2016b, The MathWorks, Natick, MA, USA) code (available on request) was designed to analyze the CSV files. In the analysis, mean and standard deviation (s.d.) of all the pixels of a cell were calculated. The pixel intensity that was greater than the mean+2 s.d. was selected. A region of the image where no cell was present was chosen as the background and the average pixel intensity of the background region was subtracted from the selected pixels of the cell. The signal intensity for each of these background subtracted pixels was normalized to the peak value which was set to 1. The sum of these normalized pixels was used to represent each cell. Over 60 cells were measured for each sample.

Time-lapse microscopy images were processed in ImageJ. Grayscale fluorescence images were converted into maximum intensity projection and inverted. Quantitation of timing of Cdc42p clustering was performed as described (Lai et al., 2018; McClure et al., 2016) with following modifications. Threshold was applied to the 16-bit grayscale image to highlight cells and converted to binary image. Any merged cells were separated using the watershed plugin after applying a Gaussian Blur filter with sigma value of 2. Using *Analyze Particles* tab, the binary image was used to analyze the grayscale image to calculate mean intensity and s.d. of each cell. CV was then calculated from the mean and s.d., and plotted as a function of time.

Kymographs were made on inverted maximum intensity projection images. Brightness and contrast were adjusted uniformly for each time frame and each strain. *Line* tool with pixel width of 1 was used to define the ROI and *Reslice* tool was used to generate slices for each time frame.

Bioinformatics and statistical analysis

GO term analysis (Ashburner et al., 2000) was performed using the Gene Ontology enRIchment analysis and visuaLizAtion algorithm (GOrilla) (Eden et al., 2007, 2009) using the two unranked lists mode. Genes encoding proteins associated with cell polarity were identified by GO term analysis (Ashburner et al., 2000; GO:0000282, cellular bud site selection; GO:0030010, establishment of cell polarity; GO:0031106, septin ring organization; GO:0006887, exocytosis; GO:0007120, axial cellular bud site selection; GO0007121, bipolar cellular bud site selection; GO:0030427, site of polarized growth). GO terms and descriptions come from SGD (http://www.yeastgenome.org). Statistical significance for pairwise comparisons was performed using Student's *t*-test in Microsoft Excel. For multiple comparisons, one-way ANOVA with Tukey's test was performed in Minitab (www.minitab.com).

Acknowledgements

We thank Matthias Peter (ETH Zürich), D. Lew (Duke University), John Pringle (Stanford University), Rong Li (Johns Hopkins University), Charlie Boone (University of Toronto), Alan Davidson (University of Toronto), Scott Emr (Cornell University), Peter Novick (Yale University), Erfei Bi (University of Pennsylvania) and Mike Yu (SUNY-Buffalo) for providing strains and/or plasmids. We also thank Steve Free (SUNY-Buffalo) for comments. Karnesh Jain (University of North Dakota) wrote the MATLAB code for quantifying Gic2p-PBD-tdTomato signal. Nadia Vadiae, Heather Dionne, Marysa Notaro, Pu Zheng, Minakshi Mukherjee, Matt Vandermeulen and Shally Lin helped with experiments.

Competing interests

The authors declare no competing or financial interests.

Author contributions

Conceptualization: A.P., P.J.C.; Methodology: A.P.; Validation: A.P.; Formal analysis: A.P., J.C., A.J.S.; Investigation: A.P., A.J.S.; Resources: A.P., A.J.S., P.J.C.; Writing - original draft: A.P., P.J.C.; Writing - review & editing: A.P., P.J.C.; Supervision: P.J.C.; Project administration: P.J.C.; Funding acquisition: P.J.C.

Funding

Attendance at the 18th annual workshop on FLIM and FRET microscopy at W.M. Keck Center for Cellular Imaging at the University of Virginia (hosted by Ammasi Periasamy), came from a travel award from the Histochemical Society (for A.P.). The work was supported from a grant from the National Institutes of Health (GM 098629). Deposited in PMC for release after 12 months.

Supplementary information

Supplementary information available online at
http://jcs.biologists.org/lookup/doi/10.1242/jcs.241513.supplemental

Peer review history

The peer review history is available online at
https://jcs.biologists.org/lookup/doi/10.1242/jcs.241513.reviewer-comments.pdf

References

Adhikari, H. and Cullen, P. J. (2014). Metabolic respiration induces AMPK- and Ire1p-dependent activation of the p38-type HOG MAPK pathway. *PLoS Genet.* **10**, e1004734. doi:10.1371/journal.pgen.1004734

Adhikari, H., Vadaie, N., Chow, J., Caccamise, L. M., Chavel, C. A., Li, B., Bowitch, A., Stefan, C. J. and Cullen, P. J. (2015). Role of the unfolded protein response in regulating the mucin-dependent filamentous-growth mitogen-activated protein kinase pathway. *Mol. Cell. Biol.* **35**, 1414-1432. doi:10.1128/MCB.01501-14

Arkowitz, R. A. and Iglesias, P. A. (2008). Basic principles of polarity establishment and maintenance. Conference on Mechanisms of Cell Polarity. *EMBO Rep.* **9**, 847-852. doi:10.1038/embor.2008.164

Asakura, T., Sasaki, T., Nagano, F., Satoh, A., Obaishi, H., Nishioka, H., Imamura, H., Hotta, K., Tanaka, K., Nakanishi, H. et al. (1998). Isolation and characterization of a novel actin filament-binding protein from *Saccharomyces cerevisiae*. *Oncogene* **16**, 121-130. doi:10.1038/sj.onc.1201487

Ashburner, M., Ball, C. A., Blake, J. A., Botstein, D., Butler, H., Cherry, J. M., Davis, A. P., Dolinski, K., Dwight, S. S., Eppig, J. T. et al. (2000). Gene ontology: tool for the unification of biology. The Gene Ontology Consortium. *Nat. Genet.* **25**, 25-29. doi:10.1038/75556

Bardwell, L., Cook, J. G., Zhu-Shimoni, J. X., Voora, D. and Thorner, J. (1998). Differential regulation of transcription: repression by unactivated mitogen-activated protein kinase Kss1 requires the Dig1 and Dig2 proteins. *Proc. Natl. Acad. Sci. USA* **95**, 15400-15405. doi:10.1073/pnas.95.26.15400

Bassard, J.-E. and Halkier, B. A. (2018). How to prove the existence of metabolons? *Phytochem. Rev.* **17**, 211-227. doi:10.1007/s11101-017-9509-1

Basu, S., González, B., Li, B., Kimble, G., Kozminski, K. G. and Cullen, P. J. (2020). Functions for Cdc42p BEM adaptors in regulating a differentiation-type MAP kinase pathway. *Mol. Biol. Cell* **31**, 491-510. doi:10.1091/mbc.E19-08-0441

Basu, S., Vadaie, N., Prabhakar, A., Li, B., Adhikari, H., Pitoniak, A., Chow, J., Chavel, C. A. and Cullen, P. J. (2016). Spatial landmarks regulate a Cdc42-dependent MAPK pathway to control differentiation and the response to positional compromise. *Proc. Natl. Acad. Sci. USA* **113**, E2019-E2028. doi:10.1073/pnas.1522679113

Baudin, A., Ozier-Kalogeropoulos, O., Denouel, A., Lacroute, F. and Cullin, C. (1993). A simple and efficient method for direct gene deletion in *Saccharomyces cerevisiae*. *Nucleic Acids Res.* **21**, 3329-3330. doi:10.1093/nar/21.14.3329

Bauer, Y., Knechtle, P., Wendland, J., Helfer, H. and Philippsen, P. (2004). A Ras-like GTPase is involved in hyphal growth guidance in the filamentous fungus *Ashbya gossypii*. *Mol. Biol. Cell* **15**, 4622-4632. doi:10.1091/mbc.e04-02-0104

Bender, A. and Pringle, J. R. (1989). Multicopy suppression of the cdc24 budding defect in yeast by CDC42 and three newly identified genes including the ras-related gene RSR1. *Proc. Natl. Acad. Sci. USA* **86**, 9976-9980. doi:10.1073/pnas.86.24.9976

Bender, A. and Pringle, J. R. (1991). Use of a screen for synthetic lethal and multicopy suppressee mutants to identify two new genes involved in morphogenesis in *Saccharomyces cerevisiae*. *Mol. Cell. Biol.* **11**, 1295-1305. doi:10.1128/MCB.11.3.1295

Bender, A. and Pringle, J. R. (1992). A Ser/Thr-rich multicopy suppressor of a cdc24 bud emergence defect. *Yeast* **8**, 315-323. doi:10.1002/yea.320080409

Bender, L., Lo, H. S., Lee, H., Kokojan, V., Peterson, V. and Bender, A. (1996). Associations among PH and SH3 domain-containing proteins and Rho-type GTPases in yeast. *J. Cell Biol.* **133**, 879-894. doi:10.1083/jcb.133.4.879

Bendezú, F. O. and Martin, S. G. (2013). Cdc42 explores the cell periphery for mate selection in fission yeast. *Curr. Biol.* **23**, 42-47. doi:10.1016/j.cub.2012.10.042

Bi, E. and Park, H.-O. (2012). Cell polarization and cytokinesis in budding yeast. *Genetics* **191**, 347-387. doi:10.1534/genetics.111.132886

Bi, E., Chiavetta, J. B., Chen, H., Chen, G.-C., Chan, C. S. M. and Pringle, J. R. (2000). Identification of novel, evolutionarily conserved Cdc42p-interacting proteins and of redundant pathways linking Cdc24p and Cdc42p to actin polarization in yeast. *Mol. Biol. Cell* **11**, 773-793. doi:10.1091/mbc.11.2.773

Borneman, A. R., Gianoulis, T. A., Zhang, Z. D., Yu, H., Rozowsky, J., Seringhaus, M. R., Wang, L. Y., Gerstein, M. and Snyder, M. (2007). Divergence of transcription factor binding sites across related yeast species. *Science* **317**, 815-819. doi:10.1126/science.1140748

Breeden, L. L. (1997). α-Factor synchronization of budding yeast. *Methods Enzymol.* **283**, 332-342. doi:10.1016/S0076-6879(97)83027-3

Brewster, J. L., de Valoir, T., Dwyer, N. D., Winter, E. and Gustin, M. C. (1993). An osmosensing signal transduction pathway in yeast. *Science* **259**, 1760-1763. doi:10.1126/science.7681220

Brown, J. L., Jaquenoud, M., Gulli, M. P., Chant, J. and Peter, M. (1997). Novel Cdc42-binding proteins Gic1 and Gic2 control cell polarity in yeast. *Genes Dev.* **11**, 2972-2982. doi:10.1101/gad.11.22.2972

Brown, J. L., Stowers, L., Baer, M., Trejo, J. A., Coughlin, S. and Chant, J. (1996). Human Ste20 homologue hPAK1 links GTPases to the JNK MAP kinase pathway. *Curr. Biol.* **6**, 598-605. doi:10.1016/S0960-9822(02)00546-8

Caviston, J. P., Longtine, M., Pringle, J. R. and Bi, E. (2003). The role of Cdc42p GTPase-activating proteins in assembly of the septin ring in yeast. *Mol. Biol. Cell* **14**, 4051-4066. doi:10.1091/mbc.e03-04-0247

Caviston, J. P., Tcheperegine, S. E. and Bi, E. (2002). Singularity in budding: a role for the evolutionarily conserved small GTPase Cdc42p. *Proc. Natl. Acad. Sci. USA* **99**, 12185-12190. doi:10.1073/pnas.182370299

Cepeda-García, C. (2017). Determination of cell cycle stage and mitotic exit through the quantification of the protein levels of known mitotic regulators. *Methods Mol. Biol.* **1505**, 45-57. doi:10.1007/978-1-4939-6502-1_4

Chavel, C. A., Dionne, H. M., Birkaya, B., Joshi, J. and Cullen, P. J. (2010). Multiple signals converge on a differentiation MAPK pathway. *PLoS Genet.* **6**, e1000883. doi:10.1371/journal.pgen.1000883

Chen, G.-C., Kim, Y.-J. and Chan, C. S. M. (1997). The Cdc42 GTPase-associated proteins Gic1 and Gic2 are required for polarized cell growth in *Saccharomyces cerevisiae*. *Genes Dev.* **11**, 2958-2971. doi:10.1101/gad.11.22.2958

Chen, H., Kuo, C.-C., Kang, H., Howell, A. S., Zyla, T. R., Jin, M. and Lew, D. J. (2012). Cdc42p regulation of the yeast formin Bni1p mediated by the effector Gic2p. *Mol. Biol. Cell* **23**, 3814-3826. doi:10.1091/mbc.e12-05-0400

Chiou, J.-G., Balasubramanian, M. K. and Lew, D. J. (2017). Cell polarity in yeast. *Annu. Rev. Cell Dev. Biol.* **33**, 77-101. doi:10.1146/annurev-cellbio-100616-060856

Chiou, J.-G., Ramirez, S. A., Elston, T. C., Witelski, T. P., Schaeffer, D. G. and Lew, D. J. (2018). Principles that govern competition or co-existence in Rho-GTPase driven polarization. *PLoS Comput. Biol.* **14**, e1006095. doi:10.1371/journal.pcbi.1006095

Cho, R. J., Campbell, M. J., Winzeler, E. A., Steinmetz, L., Conway, A., Wodicka, L., Wolfsberg, T. G., Gabrielian, A. E., Landsman, D., Lockhart, D. J. et al. (1998). A genome-wide transcriptional analysis of the mitotic cell cycle. *Mol. Cell* **2**, 65-73. doi:10.1016/S1097-2765(00)80114-8

Chow, J., Dionne, H. M., Prabhakar, A., Mehrotra, A., Somboonthum, J., Gonzalez, B., Edgerton, M. and Cullen, P. J. (2019). Aggregate filamentous growth responses in yeast. *mSphere* **4**, e00702-18. doi:10.1128/mSphere.00702-18

Cid, V. J., Adamiková, L., Sánchez, M., Molina, M. and Nombela, C. (2001). Cell cycle control of septin ring dynamics in the budding yeast. *Microbiology* **147**, 1437-1450. doi:10.1099/00221287-147-6-1437

Costanzo, M., Baryshnikova, A., Bellay, J., Kim, Y., Spear, E. D., Sevier, C. S., Ding, H., Koh, J. L. Y., Toufighi, K., Mostafavi, S. et al. (2010). The genetic landscape of a cell. *Science* **327**, 425-431. doi:10.1126/science.1180823

Cross, F. R., Schroeder, L., Kruse, M. and Chen, K. C. (2005). Quantitative characterization of a mitotic cyclin threshold regulating exit from mitosis. *Mol. Biol. Cell* **16**, 2129-2138. doi:10.1091/mbc.e04-10-0897

Cullen, P. J. (2015). Evaluating yeast filamentous growth at the single-cell level. *Cold Spring Harb. Protoc.* **2015**, 272-275. doi:10.1101/pdb.prot085084

Cullen, P. J. and Sprague, G. F. Jr. (2000). Glucose depletion causes haploid invasive growth in yeast. *Proc. Natl. Acad. Sci. USA* **97**, 13619-13624. doi:10.1073/pnas.240345197

Cullen, P. J. and Sprague, G. F. Jr. (2002). The roles of bud-site-selection proteins during haploid invasive growth in yeast. *Mol. Biol. Cell* **13**, 2990-3004. doi:10.1091/mbc.e02-03-0151

Cullen, P. J., Sabbagh, W., Jr., Graham, E., Irick, M. M., van Olden, E. K., Neal, C., Delrow, J., Bardwell, L. and Sprague, G. F. Jr. (2004). A signaling mucin at the head of the Cdc42- and MAPK-dependent filamentous growth pathway in yeast. *Genes Dev.* **18**, 1695-1708. doi:10.1101/gad.1178604

Cvrckova, F., De Virgilio, C., Manser, E., Pringle, J. R. and Nasmyth, K. (1995). Ste20-like protein kinases are required for normal localization of cell growth and for cytokinesis in budding yeast. *Genes Dev.* **9**, 1817-1830. doi:10.1101/gad.9.15.1817

Daniels, C. N., Zyla, T. R. and Lew, D. J. (2018). A role for Gic1 and Gic2 in Cdc42 polarization at elevated temperature. *PLoS ONE* **13**, e0200863. doi:10.1371/journal.pone.0200863

Das, M., Drake, T., Wiley, D. J., Buchwald, P., Vavylonis, D. and Verde, F. (2012). Oscillatory dynamics of Cdc42 GTPase in the control of polarized growth. *Science* **337**, 239-243. doi:10.1126/science.1218377

Das, M., Wiley, D. J., Medina, S., Vincent, H. A., Larrea, M., Oriolo, A. and Verde, F. (2007). Regulation of cell diameter, For3p localization, and cell symmetry by fission yeast Rho-GAP Rga4p. *Mol. Biol. Cell* **18**, 2090-2101. doi:10.1091/mbc.e06-09-0883

Davenport, K. D., Williams, K. E., Ullmann, B. D. and Gustin, M. C. (1999). Activation of the *Saccharomyces cerevisiae* filamentation/invasion pathway by osmotic stress in high-osmolarity glycogen pathway mutants. *Genetics* **153**, 1091-1103.

Desai, J. V., Mitchell, A. P. and Andes, D. R. (2014). Fungal biofilms, drug resistance, and recurrent infection. *Cold Spring Harb. Perspect. Med.* **4**, a019729. doi:10.1101/cshperspect.a019729

Dinsmore, C. J. and Soriano, P. (2018). MAPK and PI3K signaling: at the crossroads of neural crest development. *Dev. Biol.* **444** Suppl. 1, S79-S97. doi:10.1016/j.ydbio.2018.02.003

Doerr, S. and Ragkousi, K. (2019). Cell polarity oscillations in mitotic epithelia. *Curr. Opin. Genet. Dev.* **57**, 47-53. doi:10.1016/j.gde.2019.07.007

Dyer, J. M., Savage, N. S., Jin, M., Zyla, T. R., Elston, T. C. and Lew, D. J. (2013). Tracking shallow chemical gradients by actin-driven wandering of the polarization site. *Curr. Biol.* **23**, 32-41. doi:10.1016/j.cub.2012.11.014

Eden, E., Lipson, D., Yogev, S. and Yakhini, Z. (2007). Discovering motifs in ranked lists of DNA sequences. *PLoS Comput. Biol.* **3**, e39. doi:10.1371/journal.pcbi.0030039

Eden, E., Navon, R., Steinfeld, I., Lipson, D. and Yakhini, Z. (2009). GOrilla: a tool for discovery and visualization of enriched GO terms in ranked gene lists. *BMC Bioinformatics* **10**, 48. doi:10.1186/1471-2105-10-48

Eluere, R., Offner, N., Varlet, I., Motteux, O., Signon, L., Picard, A., Bailly, E. and Simon, M.-N. (2007). Compartmentalization of the functions and regulation of the mitotic cyclin Clb2 in *S. cerevisiae*. *J. Cell Sci.* **120**, 702-711. doi:10.1242/jcs.03380

Evangelista, M., Blundell, K., Longtine, M. S., Chow, C. J., Adames, N., Pringle, J. R., Peter, M. and Boone, C. (1997). Bni1p, a yeast formin linking cdc42p and the actin cytoskeleton during polarized morphogenesis. *Science* **276**, 118-122. doi:10.1126/science.276.5309.118

Fares, H., Goetsch, L. and Pringle, J. R. (1996). Identification of a developmentally regulated septin and involvement of the septins in spore formation in *Saccharomyces cerevisiae*. *J. Cell Biol.* **132**, 399-411. doi:10.1083/jcb.132.3.399

Finger, F. P. and Novick, P. (1997). Sec3p is involved in secretion and morphogenesis in *Saccharomyces cerevisiae*. *Mol. Biol. Cell* **8**, 647-662. doi:10.1091/mbc.8.4.647

Finger, F. P. and Novick, P. (2000). Synthetic interactions of the post-Golgi sec mutations of *Saccharomyces cerevisiae*. *Genetics* **156**, 943-951.

Fomicheva, M., Tross, E. M. and Macara, I. G. (2020). Polarity proteins in oncogenesis. *Curr. Opin. Cell Biol.* **62**, 26-30. doi:10.1016/j.ceb.2019.07.016

Freisinger, T., Klünder, B., Johnson, J., Müller, N., Pichler, G., Beck, G., Costanzo, M., Boone, C., Cerione, R. A., Frey, E. et al. (2013). Establishment of a robust single axis of cell polarity by coupling multiple positive feedback loops. *Nat. Commun.* **4**, 1807. doi:10.1038/ncomms2795

Gancedo, J. M. (2001). Control of pseudohyphae formation in *Saccharomyces cerevisiae*. *FEMS Microbiol. Rev.* **25**, 107-123. doi:10.1111/j.1574-6976.2001.tb00573.x

Gandhi, M., Goode, B. L. and Chan, C. S. M. (2006). Four novel suppressors of gic1 gic2 and their roles in cytokinesis and polarized cell growth in

Saccharomyces cerevisiae. *Genetics* **174**, 665-678. doi:10.1534/genetics.106.058180

Gelperin, D. M., White, M. A., Wilkinson, M. L., Kon, Y., Kung, L. A., Wise, K. J., Lopez-Hoyo, N., Jiang, L., Piccirillo, S., Yu, H. et al. (2005). Biochemical and genetic analysis of the yeast proteome with a movable ORF collection. *Genes Dev.* **19**, 2816-2826. doi:10.1101/gad.1362105

Gimeno, C. J. and Fink, G. R. (1994). Induction of pseudohyphal growth by overexpression of PHD1, a *Saccharomyces cerevisiae* gene related to transcriptional regulators of fungal development. *Mol. Cell. Biol.* **14**, 2100-2112. doi:10.1128/MCB.14.3.2100

Gimeno, C. J., Ljungdahl, P. O., Styles, C. A. and Fink, G. R. (1992). Unipolar cell divisions in the yeast *S. cerevisiae* lead to filamentous growth: regulation by starvation and RAS. *Cell* **68**, 1077-1090. doi:10.1016/0092-8674(92)90079-R

Gladfelter, A. S., Bose, I., Zyla, T. R., Bardes, E. S. G. and Lew, D. J. (2002). Septin ring assembly involves cycles of GTP loading and hydrolysis by Cdc42p. *J. Cell Biol.* **156**, 315. doi:10.1083/jcb.200109062

Gladfelter, A. S., Kozubowski, L., Zyla, T. R. and Lew, D. J. (2005). Interplay between septin organization, cell cycle and cell shape in yeast. *J. Cell Sci.* **118**, 1617. doi:10.1242/jcs.02286

Gladfelter, A. S., Moskow, J. J., Zyla, T. R. and Lew, D. J. (2001). Isolation and characterization of effector-loop mutants of CDC42 in yeast. *Mol. Biol. Cell* **12**, 1239-1255. doi:10.1091/mbc.12.5.1239

Glomb, O., Wu, Y., Rieger, L., Rüthnick, D., Mulaw, M. A. and Johnsson, N. (2020). The cell polarity proteins Boi1 and Boi2 direct an actin nucleation complex to sites of exocytosis. *J. Cell Sci.* **133**, jcs.237982. doi:10.1242/jcs.237982

Goldstein, A. L. and McCusker, J. H. (1999). Three new dominant drug resistance cassettes for gene disruption in *Saccharomyces cerevisiae*. *Yeast* **15**, 1541-1553. doi:10.1002/(SICI)1097-0061(199910)15:14<1541::AID-YEA476>3.0.CO;2-K

Gratton, E., Breusegem, S., Sutin, J., Ruan, Q. and Barry, N. (2003). Fluorescence lifetime imaging for the two-photon microscope: time-domain and frequency-domain methods. *J. Biomed. Opt.* **8**, 381-390. doi:10.1117/1.1586704

Gulli, M.-P., Jaquenoud, M., Shimada, Y., Niederhäuser, G., Wiget, P. and Peter, M. (2000). Phosphorylation of the Cdc42 exchange factor Cdc24 by the PAK-like kinase Cla4 may regulate polarized growth in yeast. *Mol. Cell* **6**, 1155-1167. doi:10.1016/S1097-2765(00)00113-1

Guo, F., Hildeman, D., Tripathi, P., Velu, C. S., Grimes, H. L. and Zheng, Y. (2010). Coordination of IL-7 receptor and T-cell receptor signaling by cell-division cycle 42 in T-cell homeostasis. *Proc. Natl. Acad. Sci. USA* **107**, 18505-18510. doi:10.1073/pnas.1010249107

Hall, B. G., Acar, H., Nandipati, A. and Barlow, M. (2014). Growth rates made easy. *Mol. Biol. Evol.* **31**, 232-238. doi:10.1093/molbev/mst187

Harkins, H. A., Pagé, N., Schenkman, L. R., De Virgilio, C., Shaw, S., Bussey, H. and Pringle, J. R. (2001). Bud8p and Bud9p, proteins that may mark the sites for bipolar budding in yeast. *Mol. Biol. Cell* **12**, 2497-2518. doi:10.1091/mbc.12.8.2497

Hartwell, L. H., Culotti, J. and Reid, B. (1970). Genetic control of the cell-division cycle in yeast. I. Detection of mutants. *Proc. Natl. Acad. Sci. USA* **66**, 352-359. doi:10.1073/pnas.66.2.352

Henderson, D. J., Long, D. A. and Dean, C. H. (2018). Planar cell polarity in organ formation. *Curr. Opin. Cell Biol.* **55**, 96-103. doi:10.1016/j.ceb.2018.06.011

Hofmann, C., Shepelev, M. and Chernoff, J. (2004). The genetics of Pak. *J. Cell Sci.* **117**, 4343-4354. doi:10.1242/jcs.01392

Howell, A. S. and Lew, D. J. (2012). Morphogenesis and the cell cycle. *Genetics* **190**, 51-77. doi:10.1534/genetics.111.128314

Howell, A. S., Jin, M., Wu, C.-F., Zyla, T. R., Elston, T. C. and Lew, D. J. (2012). Negative feedback enhances robustness in the yeast polarity establishment circuit. *Cell* **149**, 322-333. doi:10.1016/j.cell.2012.03.012

Howell, A. S., Savage, N. S., Johnson, S. A., Bose, I., Wagner, A. W., Zyla, T. R., Nijhout, H. F., Reed, M. C., Goryachev, A. B. and Lew, D. J. (2009). Singularity in polarization: rewiring yeast cells to make two buds. *Cell* **139**, 731-743. doi:10.1016/j.cell.2009.10.024

Hu, Z., Killion, P. J. and Iyer, V. R. (2007). Genetic reconstruction of a functional transcriptional regulatory network. *Nat. Genet.* **39**, 683-687. doi:10.1038/ng2012

Irazoqui, J. E. and Lew, D. J. (2004). Polarity establishment in yeast. *J. Cell Sci.* **117**, 2169-2171. doi:10.1242/jcs.00953

Irazoqui, J. E., Gladfelter, A. S. and Lew, D. J. (2003). Scaffold-mediated symmetry breaking by Cdc42p. *Nat. Cell Biol.* **5**, 1062-1070. doi:10.1038/ncb1068

Irniger, S., Piatti, S., Michaelis, C. and Nasmyth, K. (1995). Genes involved in sister chromatid separation are needed for B-type cyclin proteolysis in budding yeast. *Cell* **81**, 269-278. doi:10.1016/0092-8674(95)90337-2

Iwase, M., Luo, J., Nagaraj, S., Longtine, M., Kim, H. B., Haarer, B. K., Caruso, C., Tong, Z., Pringle, J. R. and Bi, E. (2006). Role of a Cdc42p effector pathway in recruitment of the yeast septins to the presumptive bud site. *Mol. Biol. Cell* **17**, 1110-1125. doi:10.1091/mbc.e05-08-0793

Jaquenoud, M., Gulli, M.-P., Peter, K. and Peter, M. (1998). The Cdc42p effector Gic2p is targeted for ubiquitin-dependent degradation by the SCF^{Grr1} complex. *EMBO J.* **17**, 5360. doi:10.1093/emboj/17.18.5360

Jenness, D. D., Goldman, B. S. and Hartwell, L. H. (1987). *Saccharomyces cerevisiae* mutants unresponsive to alpha-factor pheromone: alpha-factor binding and extragenic suppression. *Mol. Cell. Biol.* **7**, 1311-1319. doi:10.1128/MCB.7.4.1311

Jimeno, D. and Santos, E. (2017). A new functional role uncovered for RASGRF2 in control of nuclear migration in cone photoreceptors during postnatal retinal development. *Small GTPases* **8**, 26-30. doi:10.1080/21541248.2016.1189989

Kadota, J., Yamamoto, T., Yoshiuchi, S., Bi, E. and Tanaka, K. (2004). Septin ring assembly requires concerted action of polarisome components, a PAK kinase Cla4p, and the actin cytoskeleton in *Saccharomyces cerevisiae*. *Mol. Biol. Cell* **15**, 5329-5345. doi:10.1091/mbc.e04-03-0254

Kaksonen, M., Sun, Y. and Drubin, D. G. (2003). A pathway for association of receptors, adaptors, and actin during endocytic internalization. *Cell* **115**, 475-487. doi:10.1016/S0092-8674(03)00883-3

Kang, P. J., Miller, K. E., Guegueniat, J., Beven, L. and Park, H.-O. (2018). The shared role of the Rsr1 GTPase and Gic1/Gic2 in Cdc42 polarization. *Mol. Biol. Cell* **29**, 2359-2369. doi:10.1091/mbc.E18-02-0145

Kawasaki, R., Fujimura-Kamada, K., Toi, H., Kato, H. and Tanaka, K. (2003). The upstream regulator, Rsr1p, and downstream effectors, Gic1p and Gic2p, of the Cdc42p small GTPase coordinately regulate initiation of budding in *Saccharomyces cerevisiae*. *Genes Cells* **8**, 235-250. doi:10.1046/j.1365-2443.2003.00629.x

Kim, H. B., Haarer, B. K. and Pringle, J. R. (1991). Cellular morphogenesis in the *Saccharomyces cerevisiae* cell cycle: localization of the CDC3 gene product and the timing of events at the budding site. *J. Cell Biol.* **112**, 535-544. doi:10.1083/jcb.112.4.535

Klímová, Z., Bráborec, V., Maninová, M., Čáslavský, J., Weber, M. J. and Vomastek, T. (2016). Symmetry breaking in spreading RAT2 fibroblasts requires the MAPK/ERK pathway scaffold RACK1 that integrates FAK, p190A-RhoGAP and ERK2 signaling. *Biochim. Biophys. Acta* **1863**, 2189-2200. doi:10.1016/j.bbamcr.2016.05.013

Kozubowski, L., Saito, K., Johnson, J. M., Howell, A. S., Zyla, T. R. and Lew, D. J. (2008). Symmetry-breaking polarization driven by a Cdc42p GEF-PAK complex. *Curr. Biol.* **18**, 1719-1726. doi:10.1016/j.cub.2008.09.060

Kron, S. J., Styles, C. A. and Fink, G. R. (1994). Symmetric cell division in pseudohyphae of the yeast *Saccharomyces cerevisiae*. *Mol. Biol. Cell* **5**, 1003-1022. doi:10.1091/mbc.5.9.1003

Kuczera, T., Bayram, O., Sari, F., Braus, G. H. and Irniger, S. (2010). Dissection of mitotic functions of the yeast cyclin Clb2. *Cell Cycle* **9**, 2611-2619. doi:10.4161/cc.9.13.12082

Lagree, K. and Mitchell, A. P. (2017). Fungal biofilms: inside out. *Microbiol. Spectr.* **5**, 10.1128/microbiolspec.FUNK-0024-2016. doi:10.1128/microbiolspec.FUNK-0024-2016

Lai, H., Chiou, J.-G., Zhurikhina, A., Zyla, T. R., Tsygankov, D. and Lew, D. J. (2018). Temporal regulation of morphogenetic events in *Saccharomyces cerevisiae*. *Mol. Biol. Cell* **29**, 2069-2083. doi:10.1091/mbc.E18-03-0188

Lamb, T. M. and Mitchell, A. P. (2003). The transcription factor Rim101p governs ion tolerance and cell differentiation by direct repression of the regulatory genes NRG1 and SMP1 in *Saccharomyces cerevisiae*. *Mol. Cell. Biol.* **23**, 677-686. doi:10.1128/MCB.23.2.677-686.2003

Leberer, E., Wu, C., Leeuw, T., Fourest-Lieuvin, A., Segall, J. E. and Thomas, D. Y. (1997). Functional characterization of the Cdc42p binding domain of yeast Ste20p protein kinase. *EMBO J.* **16**, 83-97. doi:10.1093/emboj/16.1.83

Lee, M. J. and Dohlman, H. G. (2008). Coactivation of G protein signaling by cell-surface receptors and an intracellular exchange factor. *Curr. Biol.* **18**, 211-215. doi:10.1016/j.cub.2008.01.007

Leitao, R. M. and Kellogg, D. R. (2017). The duration of mitosis and daughter cell size are modulated by nutrients in budding yeast. *J. Cell Biol.* **216**, 3463-3470. doi:10.1083/jcb.201609114

Lew, D. J. and Reed, S. I. (1993). Morphogenesis in the yeast cell cycle: regulation by Cdc28 and cyclins. *J. Cell Biol.* **120**, 1305-1320. doi:10.1083/jcb.120.6.1305

Liao, Y., He, F., Gong, T., Bi, E. and Gao, X.-D. (2013). Msb1 interacts with Cdc42, Boi1, and Boi2 and may coordinate Cdc42 and Rho1 functions during early stage of bud development in budding yeast. *PLoS ONE* **8**, e66321. doi:10.1371/journal.pone.0066321

Lippincott, J., Shannon, K. B., Shou, W., Deshaies, R. J. and Li, R. (2001). The Tem1 small GTPase controls actomyosin and septin dynamics during cytokinesis. *J. Cell Sci.* **114**, 1379-1386.

Liu, H., Styles, C. A. and Fink, G. R. (1993). Elements of the yeast pheromone response pathway required for filamentous growth of diploids. *Science* **262**, 1741-1744. doi:10.1126/science.8259520

Liu, Y., Zhang, T., Sun, D. and Luo, G. (2019). The Cdc42 effectors Gic1 and Gic2 regulate polarized post-Golgi secretion. *Cell Biosci.* **9**, 33. doi:10.1186/s13578-019-0295-x

Lo, H.-J., Köhler, J. R., DiDomenico, B., Loebenberg, D., Cacciapuoti, A. and Fink, G. R. (1997). Nonfilamentous *C. albicans* mutants are avirulent. *Cell* **90**, 939-949. doi:10.1016/S0092-8674(00)80358-X

Loeb, J. D., Kerentseva, T. A., Pan, T., Sepulveda-Becerra, M. and Liu, H. (1999). *Saccharomyces cerevisiae* G1 cyclins are differentially involved in invasive and pseudohyphal growth independent of the filamentation mitogen-activated protein kinase pathway. *Genetics* **153**, 1535-1546.

Longtine, M. S., McKenzie, A., III, Demarini, D. J., Shah, N. G., Wach, A., Brachat, A., Philippsen, P. and Pringle, J. R. (1998). Additional modules for versatile and economical PCR-based gene deletion and modification in *Saccharomyces cerevisiae*. *Yeast* **14**, 953-961. doi:10.1002/(SICI)1097-0061(199807)14:10<953::AID-YEA293>3.0.CO;2-U

MacIsaac, K. D., Wang, T., Gordon, D. B., Gifford, D. K., Stormo, G. D. and Fraenkel, E. (2006). An improved map of conserved regulatory sites for *Saccharomyces cerevisiae*. *BMC Bioinformatics* **7**, 113. doi:10.1186/1471-2105-7-113

Madhani, H. D. and Fink, G. R. (1997). Combinatorial control required for the specificity of yeast MAPK signaling. *Science* **275**, 1314-1317. doi:10.1126/science.275.5304.1314

Madhani, H. D., Galitski, T., Lander, E. S. and Fink, G. R. (1999). Effectors of a developmental mitogen-activated protein kinase cascade revealed by expression signatures of signaling mutants. *Proc. Natl. Acad. Sci. USA* **96**, 12530-12535. doi:10.1073/pnas.96.22.12530

Madhani, H. D., Styles, C. A. and Fink, G. R. (1997). MAP kinases with distinct inhibitory functions impart signaling specificity during yeast differentiation. *Cell* **91**, 673-684. doi:10.1016/S0092-8674(00)80454-7

Marles, J. A., Dahesh, S., Haynes, J., Andrews, B. J. and Davidson, A. R. (2004). Protein-protein interaction affinity plays a crucial role in controlling the Sho1p-mediated signal transduction pathway in yeast. *Mol. Cell* **14**, 813-823. doi:10.1016/j.molcel.2004.05.024

Martin, S. G. (2019). Molecular mechanisms of chemotropism and cell fusion in unicellular fungi. *J. Cell Sci.* **132**, jcs230706. doi:10.1242/jcs.230706

Masgrau, A., Battola, A., Sanmartin, T., Pryszcz, L. P., Gabaldón, T. and Mendoza, M. (2017). Distinct roles of the polarity factors Boi1 and Boi2 in the control of exocytosis and abscission in budding yeast. *Mol. Biol. Cell* **28**, 3082-3094. doi:10.1091/mbc.e17-06-0404

McCaffrey, G., Clay, F. J., Kelsay, K. and Sprague, G. F. Jr. (1987). Identification and regulation of a gene required for cell fusion during mating of the yeast *Saccharomyces cerevisiae*. *Mol. Cell. Biol.* **7**, 2680-2690. doi:10.1128/MCB.7.8.2680

McClure, A. W., Wu, C.-F., Johnson, S. A. and Lew, D. J. (2016). Imaging polarization in budding yeast. *Methods Mol. Biol.* **1407**, 13-23. doi:10.1007/978-1-4939-3480-5_2

McCormack, J., Welsh, N. J. and Braga, V. M. M. (2013). Cycling around cell-cell adhesion with Rho GTPase regulators. *J. Cell Sci.* **126**, 379-391. doi:10.1242/jcs.097923

Meitinger, F., Khmelinskii, A., Morlot, S., Kurtulmus, B., Palani, S., Andres-Pons, A., Hub, B., Knop, M., Charvin, G. and Pereira, G. (2014). A memory system of negative polarity cues prevents replicative aging. *Cell* **159**, 1056-1069. doi:10.1016/j.cell.2014.10.014

Meitinger, F., Richter, H., Heisel, S., Hub, B., Seufert, W. and Pereira, G. (2013). A safeguard mechanism regulates Rho GTPases to coordinate cytokinesis with the establishment of cell polarity. *PLoS Biol.* **11**, e1001495. doi:10.1371/journal.pbio.1001495

Miller, K. E., Lo, W.-C., Chou, C.-S. and Park, H.-O. (2019). Temporal regulation of cell polarity via the interaction of the Ras GTPase Rsr1 and the scaffold protein Bem1. *Mol. Biol. Cell* **30**, 2537-2616. doi:10.1091/mbc.E19-02-0106

Miller, K. E., Lo, W.-C., Lee, M. E., Kang, P. J. and Park, H.-O. (2017). Fine-tuning the orientation of the polarity axis by Rga1, a Cdc42 GTPase-activating protein. *Mol. Biol. Cell* **28**, 3773-3788. doi:10.1091/mbc.e17-01-0074

Moran, K. D., Kang, H., Araujo, A. V., Zyla, T. R., Saito, K., Tsygankov, D. and Lew, D. J. (2019). Cell-cycle control of cell polarity in yeast. *J. Cell Biol.* **218**, 171. doi:10.1083/jcb.201806196

Mösch, H.-U., Kübler, E., Krappmann, S., Fink, G. R. and Braus, G. H. (1999). Crosstalk between the Ras2p-controlled mitogen-activated protein kinase and cAMP pathways during invasive growth of *Saccharomyces cerevisiae*. *Mol. Biol. Cell* **10**, 1325-1335. doi:10.1091/mbc.10.5.1325

Mosch, H. U., Roberts, R. L. and Fink, G. R. (1996). Ras2 signals via the Cdc42/Ste20/mitogen-activated protein kinase module to induce filamentous growth in *Saccharomyces cerevisiae*. *Proc. Natl. Acad. Sci. USA* **93**, 5352-5356. doi:10.1073/pnas.93.11.5352

Nern, A. and Arkowitz, R. A. (2000). G proteins mediate changes in cell shape by stabilizing the axis of polarity. *Mol. Cell* **5**, 853-864. doi:10.1016/S1097-2765(00)80325-1

Nishimura, A., Yamamoto, K., Oyama, M., Kozuka-Hata, H., Saito, H. and Tatebayashi, K. (2016). Scaffold protein Ahk1, which associates with Hkr1, Sho1, Ste11, and Pbs2, inhibits cross talk signaling from the Hkr1 osmosensor to the Kss1 mitogen-activated protein kinase. *Mol. Cell. Biol.* **36**, 1109-1123. doi:10.1128/MCB.01017-15

Noguchi, S., Saito, A. and Nagase, T. (2018). YAP/TAZ signaling as a molecular link between fibrosis and cancer. *Int. J. Mol. Sci.* **19**, 3674. doi:10.3390/ijms19113674

Okada, S., Leda, M., Hanna, J., Savage, N. S., Bi, E. and Goryachev, A. B. (2013). Daughter cell identity emerges from the interplay of Cdc42, septins, and exocytosis. *Dev. Cell* **26**, 148-161. doi:10.1016/j.devcel.2013.06.015

Okada, S., Lee, M. E., Bi, E. and Park, H.-O. (2017). Probing Cdc42 polarization dynamics in budding yeast using a biosensor. *Methods Enzymol.* **589**, 171-190. doi:10.1016/bs.mie.2017.01.011

Osterlund, E. J., Liu, Q. and Andrews, D. W. (2015). The use of FLIM-FRET for the detection of mitochondria-associated protein interactions. *Methods Mol. Biol.* **1264**, 395-419. doi:10.1007/978-1-4939-2257-4_34

Padilla-Parra, S., Audugé, N., Tramier, M. and Coppey-Moisan, M. (2015). Time-domain fluorescence lifetime imaging microscopy: a quantitative method to follow transient protein-protein interactions in living cells. *Cold Spring Harb. Protoc.* **2015**, 508-521. doi:10.1101/pdb.top086249

Pan, X., Harashima, T. and Heitman, J. (2000). Signal transduction cascades regulating pseudohyphal differentiation of *Saccharomyces cerevisiae*. *Curr. Opin. Microbiol.* **3**, 567-572. doi:10.1016/S1369-5274(00)00142-9

Papa, S., Choy, P. M. and Bubici, C. (2019). The ERK and JNK pathways in the regulation of metabolic reprogramming. *Oncogene* **38**, 2223-2240. doi:10.1038/s41388-018-0582-8

Pei, D., Shu, X., Gassama-Diagne, A. and Thiery, J. P. (2019). Mesenchymal-epithelial transition in development and reprogramming. *Nat. Cell Biol.* **21**, 44-53. doi:10.1038/s41556-018-0195-z

Periasamy, A. and Clegg, R. M. (2009). *FLIM Microscopy in Biology and Medicine*: CRC Press.

Peter, M., Neiman, A. M., Park, H. O., van Lohuizen, M. and Herskowitz, I. (1996). Functional analysis of the interaction between the small GTP binding protein Cdc42 and the Ste20 protein kinase in yeast. *EMBO J.* **15**, 7046-7059. doi:10.1002/j.1460-2075.1996.tb01096.x

Piccirillo, S. and Honigberg, S. M. (2011). Yeast colony embedding method. *J. Vis. Exp.* **49**, e2510. doi:10.3791/2510

Piroli, M. E., Blanchette, J. O. and Jabbarzadeh, E. (2019). Polarity as a physiological modulator of cell function. *Front. Biosci.* **24**, 451-462. doi:10.2741/4728

Pitoniak, A., Birkaya, B., Dionne, H. M., Vadaie, N. and Cullen, P. J. (2009). The signaling mucins Msb2 and Hkr1 differentially regulate the filamentation mitogen-activated protein kinase pathway and contribute to a multimodal response. *Mol. Biol. Cell* **20**, 3101-3114. doi:10.1091/mbc.e08-07-0760

Pitoniak, A., Chavel, C. A., Chow, J., Smith, J., Camara, D., Karunanithi, S., Li, B., Wolfe, K. H. and Cullen, P. J. (2015). Cdc42p-interacting protein Bem4p regulates the filamentous-growth mitogen-activated protein kinase pathway. *Mol. Cell. Biol.* **35**, 417-436. doi:10.1128/MCB.00850-14

Pringle, J. R., Bi, E., Harkins, H. A., Zahner, J. E., De Virgilio, C., Chant, J., Corrado, K. and Fares, H. (1995). Establishment of cell polarity in yeast. *Cold Spring Harb. Symp. Quant. Biol.* **60**, 729-744. doi:10.1101/SQB.1995.060.01.079

Pruyne, D. and Bretscher, A. (2000a). Polarization of cell growth in yeast. *J. Cell Sci.* **113**, 571-585.

Pruyne, D. and Bretscher, A. (2000b). Polarization of cell growth in yeast. I. Establishment and maintenance of polarity states. *J. Cell Sci.* **113**, 365-375.

Raman, M., Chen, W. and Cobb, M. H. (2007). Differential regulation and properties of MAPKs. *Oncogene* **26**, 3100-3112. doi:10.1038/sj.onc.1210392

Richardson, H., Lew, D. J., Henze, M., Sugimoto, K. and Reed, S. I. (1992). Cyclin-B homologs in *Saccharomyces cerevisiae* function in S phase and in G2. *Genes Dev.* **6**, 2021-2034. doi:10.1101/gad.6.11.2021

Richman, T. J. and Johnson, D. I. (2000). *Saccharomyces cerevisiae* cdc42p GTPase is involved in preventing the recurrence of bud emergence during the cell cycle. *Mol. Cell. Biol.* **20**, 8548-8559. doi:10.1128/MCB.20.22.8548-8559.2000

Riedl, J., Crevenna, A. H., Kessenbrock, K., Yu, J. H., Neukirchen, D., Bista, M., Bradke, F., Jenne, D., Holak, T. A., Werb, Z. et al. (2008). Lifeact: a versatile marker to visualize F-actin. *Nat. Methods* **5**, 605-607. doi:10.1038/nmeth.1220

Roberts, R. L. and Fink, G. R. (1994). Elements of a single MAP kinase cascade in *Saccharomyces cerevisiae* mediate two developmental programs in the same cell type: mating and invasive growth. *Genes Dev.* **8**, 2974-2985. doi:10.1101/gad.8.24.2974

Roberts, C. J., Nelson, B., Marton, M. J., Stoughton, R., Meyer, M. R., Bennett, H. A., He, Y. D., Dai, H., Walker, W. L., Hughes, T. R. et al. (2000). Signaling and circuitry of multiple MAPK pathways revealed by a matrix of global gene expression profiles. *Science* **287**, 873-880. doi:10.1126/science.287.5454.873

Rose, M. D., Winston, F. and Hieter, P. (1990). *Methods in Yeast Genetics*. Cold Spring Harbor, NY: Cold Spring Harbor Laboratory Press.

Rupp, S., Summers, E., Lo, H.-J., Madhani, H. and Fink, G. (1999). MAP kinase and cAMP filamentation signaling pathways converge on the unusually large promoter of the yeast FLO11 gene. *EMBO J.* **18**, 1257-1269. doi:10.1093/emboj/18.5.1257

Sabbagh, W., Jr., Flatauer, L. J., Bardwell, A. J. and Bardwell, L. (2001). Specificity of MAP kinase signaling in yeast differentiation involves transient versus sustained MAPK activation. *Mol. Cell* **8**, 683-691. doi:10.1016/S1097-2765(01)00322-7

Sadian, Y., Gatsogiannis, C., Patasi, C., Hofnagel, O., Goody, R. S., Farkašovský, M. and Raunser, S. (2013). The role of Cdc42 and Gic1 in the regulation of septin filament formation and dissociation. *eLife* **2**, e01085. doi:10.7554/eLife.01085

Saito, H. (2010). Regulation of cross-talk in yeast MAPK signaling pathways. *Curr. Opin. Microbiol.* **13**, 677-683. doi:10.1016/j.mib.2010.09.001
Sambrook, J., Fritsch, E. F. and Maniatis, T. (1989). *Molecular Cloning: A Laboratory Manual*. Cold Spring Harbor, NY: Cold Spring Harbor Laboratory Press.
Schneider, B. L., Seufert, W., Steiner, B., Yang, Q. H. and Futcher, A. B. (1995). Use of polymerase chain reaction epitope tagging for protein tagging in *Saccharomyces cerevisiae*. *Yeast* **11**, 1265-1274. doi:10.1002/yea.320111306
Sherer, L. A., Zweifel, M. E. and Courtemanche, N. (2018). Dissection of two parallel pathways for formin-mediated actin filament elongation. *J. Biol. Chem.* **293**, 17917-17928. doi:10.1074/jbc.RA118.004845
Si, H., Rittenour, W. R. and Harris, S. D. (2016). Roles of *Aspergillus nidulans* Cdc42/Rho GTPase regulators in hyphal morphogenesis and development. *Mycologia* **108**, 543-555. doi:10.3852/15-232
Sikorski, R. S. and Hieter, P. (1989). A system of shuttle vectors and yeast host strains designed for efficient manipulation of DNA in *Saccharomyces cerevisiae*. *Genetics* **122**, 19-27.
Simon, M.-N., De Virgilio, C., Souza, B., Pringle, J. R., Abo, A. and Reed, S. I. (1995). Role for the Rho-family GTPase Cdc42 in yeast mating-pheromone signal pathway. *Nature* **376**, 702-705. doi:10.1038/376702a0
Skinner, S. O., Sepúlveda, L. A., Xu, H. and Golding, I. (2013). Measuring mRNA copy number in individual *Escherichia coli* cells using single-molecule fluorescent *in situ* hybridization. *Nat. Protoc.* **8**, 1100-1113. doi:10.1038/nprot.2013.066
Smith, G. R., Givan, S. A., Cullen, P. and Sprague, G. F. Jr.. (2002). GTPase-activating proteins for Cdc42. *Eukaryot. Cell* **1**, 469-480. doi:10.1128/EC.1.3.469-480.2002
Smith, S. E., Rubinstein, B., Mendes Pinto, I., Slaughter, B. D., Unruh, J. R. and Li, R. (2013). Independence of symmetry breaking on Bem1-mediated autocatalytic activation of Cdc42. *J. Cell Biol.* **202**, 1091-1106. doi:10.1083/jcb.201304180
Sopko, R., Huang, D., Preston, N., Chua, G., Papp, B., Kafadar, K., Snyder, M., Oliver, S. G., Cyert, M., Hughes, T. R. et al. (2006). Mapping pathways and phenotypes by systematic gene overexpression. *Mol. Cell* **21**, 319-330. doi:10.1016/j.molcel.2005.12.011
Spellman, P. T., Sherlock, G., Zhang, M. Q., Iyer, V. R., Anders, K., Eisen, M. B., Brown, P. O., Botstein, D. and Futcher, B. (1998). Comprehensive identification of cell cycle-regulated genes of the yeast *Saccharomyces cerevisiae* by microarray hybridization. *Mol. Biol. Cell* **9**, 3273-3297. doi:10.1091/mbc.9.12.3273
Stevenson, B. J., Rhodes, N., Errede, B. and Sprague, G. F. Jr.. (1992). Constitutive mutants of the protein kinase STE11 activate the yeast pheromone response pathway in the absence of the G protein. *Genes Dev.* **6**, 1293-1304. doi:10.1101/gad.6.7.1293
Sun, Y. and Periasamy, A. (2015). Localizing protein-protein interactions in living cells using fluorescence lifetime imaging microscopy. *Methods Mol. Biol.* **1251**, 83-107. doi:10.1007/978-1-4939-2080-8_6
Sun, Y., Day, R. N. and Periasamy, A. (2011). Investigating protein-protein interactions in living cells using fluorescence lifetime imaging microscopy. *Nat. Protoc.* **6**, 1324-1340. doi:10.1038/nprot.2011.364
Taciak, B., Pruszynska, I., Kiraga, L., Bialasek, M. and Krol, M. (2018). Wnt signaling pathway in development and cancer. *J. Physiol. Pharmacol.* **69**, 10.26402/jpp.2018.2.07. doi:10.26402/jpp.2018.2.07
Taheri, N., Kohler, T., Braus, G. H. and Mosch, H. U. (2000). Asymmetrically localized Bud8p and Bud9p proteins control yeast cell polarity and development. *EMBO J.* **19**, 6686-6696. doi:10.1093/emboj/19.24.6686
Takahashi, S. and Pryciak, P. M. (2007). Identification of novel membrane-binding domains in multiple yeast Cdc42 effectors. *Mol. Biol. Cell* **18**, 4945-4956. doi:10.1091/mbc.e07-07-0676
Tatebayashi, K., Tanaka, K., Yang, H.-Y., Yamamoto, K., Matsushita, Y., Tomida, T., Imai, M. and Saito, H. (2007). Transmembrane mucins Hkr1 and Msb2 are putative osmosensors in the SHO1 branch of yeast HOG pathway. *EMBO J.* **26**, 3521-3533. doi:10.1038/sj.emboj.7601796
Tatebayashi, K., Yamamoto, K., Tanaka, K., Tomida, T., Maruoka, T., Kasukawa, E. and Saito, H. (2006). Adaptor functions of Cdc42, Ste50, and Sho1 in the yeast osmoregulatory HOG MAPK pathway. *EMBO J.* **25**, 3033-3044. doi:10.1038/sj.emboj.7601192
Tong, Z., Gao, X.-D., Howell, A. S., Bose, I., Lew, D. J. and Bi, E. (2007). Adjacent positioning of cellular structures enabled by a Cdc42 GTPase-activating protein-mediated zone of inhibition. *J. Cell Biol.* **179**, 1375-1384. doi:10.1083/jcb.200705160
Vadaie, N., Dionne, H., Akajagbor, D. S., Nickerson, S. R., Krysan, D. J. and Cullen, P. J. (2008). Cleavage of the signaling mucin Msb2 by the aspartyl protease Yps1 is required for MAPK activation in yeast. *J. Cell Biol.* **181**, 1073-1081. doi:10.1083/jcb.200704079
van der Felden, J., Weisser, S., Bruckner, S., Lenz, P. and Mosch, H.-U. (2014). The transcription factors Tec1 and Ste12 interact with coregulators Msa1 and Msa2 to activate adhesion and multicellular development. *Mol. Cell. Biol.* **34**, 2283-2293. doi:10.1128/MCB.01599-13
Venters, B. J., Wachi, S., Mavrich, T. N., Andersen, B. E., Jena, P., Sinnamon, A. J., Jain, P., Rolleri, N. S., Jiang, C., Hemeryck-Walsh, C. et al. (2011). A comprehensive genomic binding map of gene and chromatin regulatory proteins in Saccharomyces. *Mol. Cell* **41**, 480-492. doi:10.1016/j.molcel.2011.01.015
Wäsch, R. and Cross, F. R. (2002). APC-dependent proteolysis of the mitotic cyclin Clb2 is essential for mitotic exit. *Nature* **418**, 556-562. doi:10.1038/nature00856
Wedlich-Soldner, R., Altschuler, S., Wu, L. and Li, R. (2003). Spontaneous cell polarization through actomyosin-based delivery of the Cdc42 GTPase. *Science* **299**, 1231-1235. doi:10.1126/science.1080944
Wedlich-Soldner, R., Wai, S. C., Schmidt, T. and Li, R. (2004). Robust cell polarity is a dynamic state established by coupling transport and GTPase signaling. *J. Cell Biol.* **166**, 889-900. doi:10.1083/jcb.200405061
Winkler, A., Arkind, C., Mattison, C. P., Burkholder, A., Knoche, K. and Ota, I. (2002). Heat stress activates the yeast high-osmolarity glycerol mitogen-activated protein kinase pathway, and protein tyrosine phosphatases are essential under heat stress. *Eukaryot. Cell* **1**, 163-173. doi:10.1128/EC.1.2.163-173.2002
Wittenberg, C. and Reed, S. I. (2005). Cell cycle-dependent transcription in yeast: promoters, transcription factors, and transcriptomes. *Oncogene* **24**, 2746-2755. doi:10.1038/sj.onc.1208606
Woods, B. and Lew, D. J. (2019). Polarity establishment by Cdc42: key roles for positive feedback and differential mobility. *Small GTPases* **10**, 130-137. doi:10.1080/21541248.2016.1275370
Wu, X. and Jiang, Y. W. (2005). Possible integration of upstream signals at Cdc42 in filamentous differentiation of *S. cerevisiae*. *Yeast* **22**, 1069-1077. doi:10.1002/yea.1294
Wu, X., Quondamatteo, F., Lefever, T., Czuchra, A., Meyer, H., Chrostek, A., Paus, R., Langbein, L. and Brakebusch, C. (2006). Cdc42 controls progenitor cell differentiation and beta-catenin turnover in skin. *Genes Dev.* **20**, 571-585. doi:10.1101/gad.361406
Yang, H.-C. and Pon, L. A. (2002). Actin cable dynamics in budding yeast. *Proc. Natl. Acad. Sci. USA* **99**, 751-756. doi:10.1073/pnas.022462899
Yang, L., Wang, L., Geiger, H., Cancelas, J. A., Mo, J. and Zheng, Y. (2007). Rho GTPase Cdc42 coordinates hematopoietic stem cell quiescence and niche interaction in the bone marrow. *Proc. Natl. Acad. Sci. USA* **104**, 5091-5096. doi:10.1073/pnas.0610819104
Yoon, S. and Seger, R. (2006). The extracellular signal-regulated kinase: multiple substrates regulate diverse cellular functions. *Growth Factors* **24**, 21-44. doi:10.1080/02699050500284218
Yuzyuk, T. and Amberg, D. C. (2003). Actin recovery and bud emergence in osmotically stressed cells requires the conserved actin interacting mitogen-activated protein kinase Ssk2p/MTK1 and the scaffold protein Spa2p. *Mol. Biol. Cell* **14**, 3013-3026. doi:10.1091/mbc.e02-11-0747
Zanelli, C. F. and Valentini, S. R. (2005). Pkc1 acts through Zds1 and Gic1 to suppress growth and cell polarity defects of a yeast eIF5A mutant. *Genetics* **171**, 1571-1581. doi:10.1534/genetics.105.048082
Zarrinpar, A., Bhattacharyya, R. P., Nittler, M. P. and Lim, W. A. (2004). Sho1 and Pbs2 act as coscaffolds linking components in the yeast high osmolarity MAP kinase pathway. *Mol. Cell* **14**, 825-832. doi:10.1016/j.molcel.2004.06.011
Zihni, C. and Terry, S. J. (2015). RhoGTPase signalling at epithelial tight junctions: bridging the GAP between polarity and cancer. *Int. J. Biochem. Cell Biol.* **64**, 120-125. doi:10.1016/j.biocel.2015.02.020

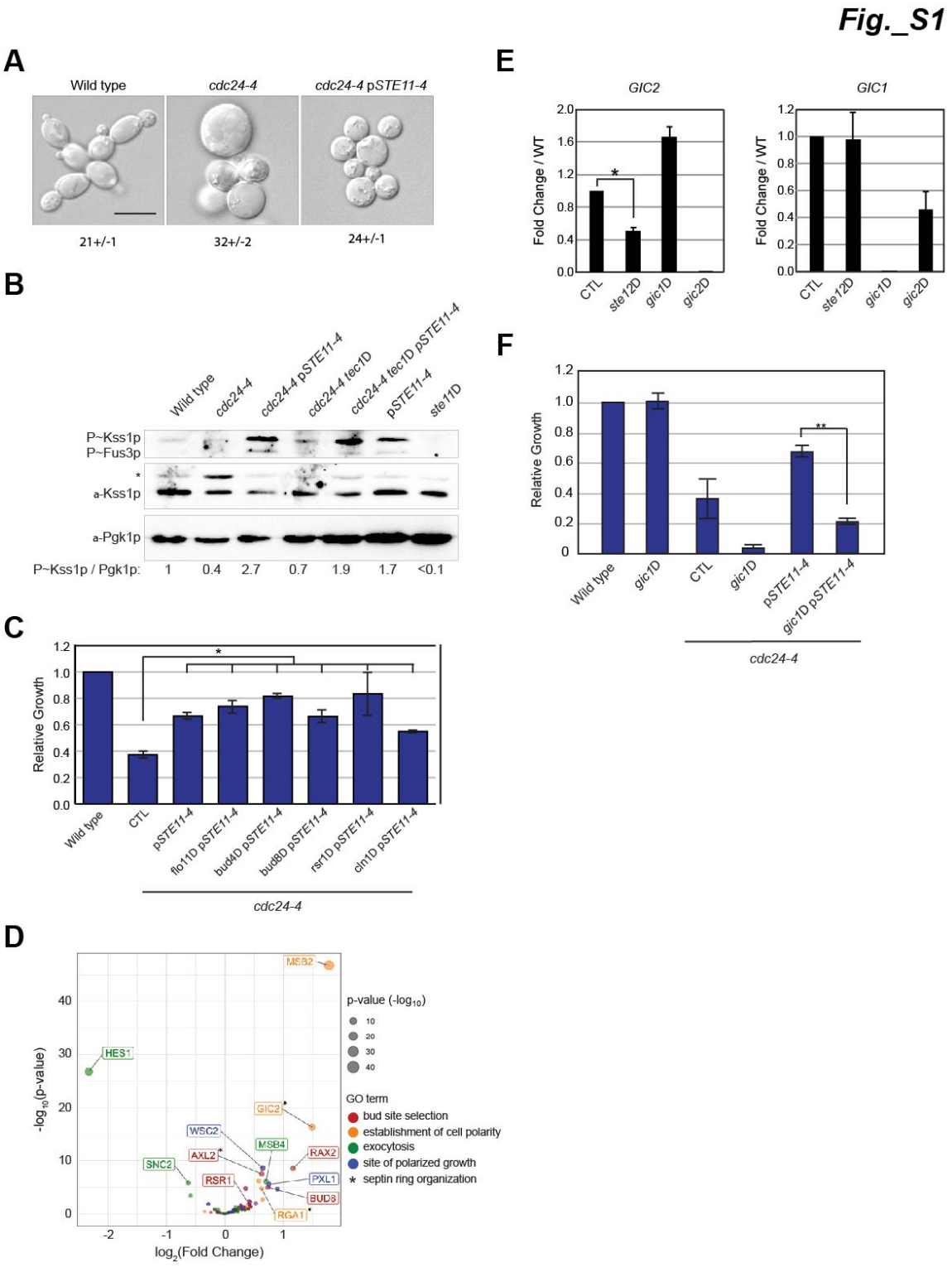

Figure S1. Effect of fMAPK pathway on growth defect of the *cdc24-4* mutant. (**A**) Typical example of cells of the indicated strains by DIC at 100X. Bar, 10 microns. Numbers refer to surface area of cells measured in Image J. Error shows the standard

error of mean for three separate trials. 50 cells were counted in each trial. The differences in the values compared to wild type are significant. p-value < 0.01. (**B**) Immunoblot analysis. p44/42 recognizes P~ERK, including P~Kss1p and P~Fus3p as indicated. Pgk1p control for protein levels. Numbers refer to the ratio of P~Kss1p to Pgk1p relative to wild type. **(C)** Role of the fMAPK pathway (p*STE11-4*) on the growth of the *cdc24-4* and indicated mutant combinations. CTL, plasmid pRS316. See Fig.1B for details. (**D**) Volcano plot showing the distribution of fMAPK pathway target genes associated with cell polarity. Genes were graphed by $\log_2$fold change (X-axis, $|\log_2\text{fold change}| > 0.585$) and p-value (Y-axis, $< 10^{-5}$). GO terms are indicated by color. p-value <0.0001 for the genes shown. Asterisk denotes multiple GO term designations. (**E**) Quantitative PCR analysis showing relative fold changes in the mRNA levels of *GIC2* (left) and *GIC1* (right) in indicated strains. Error bars represent standard deviation among 2 replicates. Asterisk, p-value < 0.05. CTL, wild type. Other polarity targets genes were confirmed in [(Adhikari and Cullen, 2014) for *RSR1, BUD8,* and *RAX2*, and (Cullen et al., 2004) for *MSB2*]. (**F**) Growth assay of wild type and *GIC1* mutant combinations at 37°C. CTL, plasmid pRS316.

Fig._S2

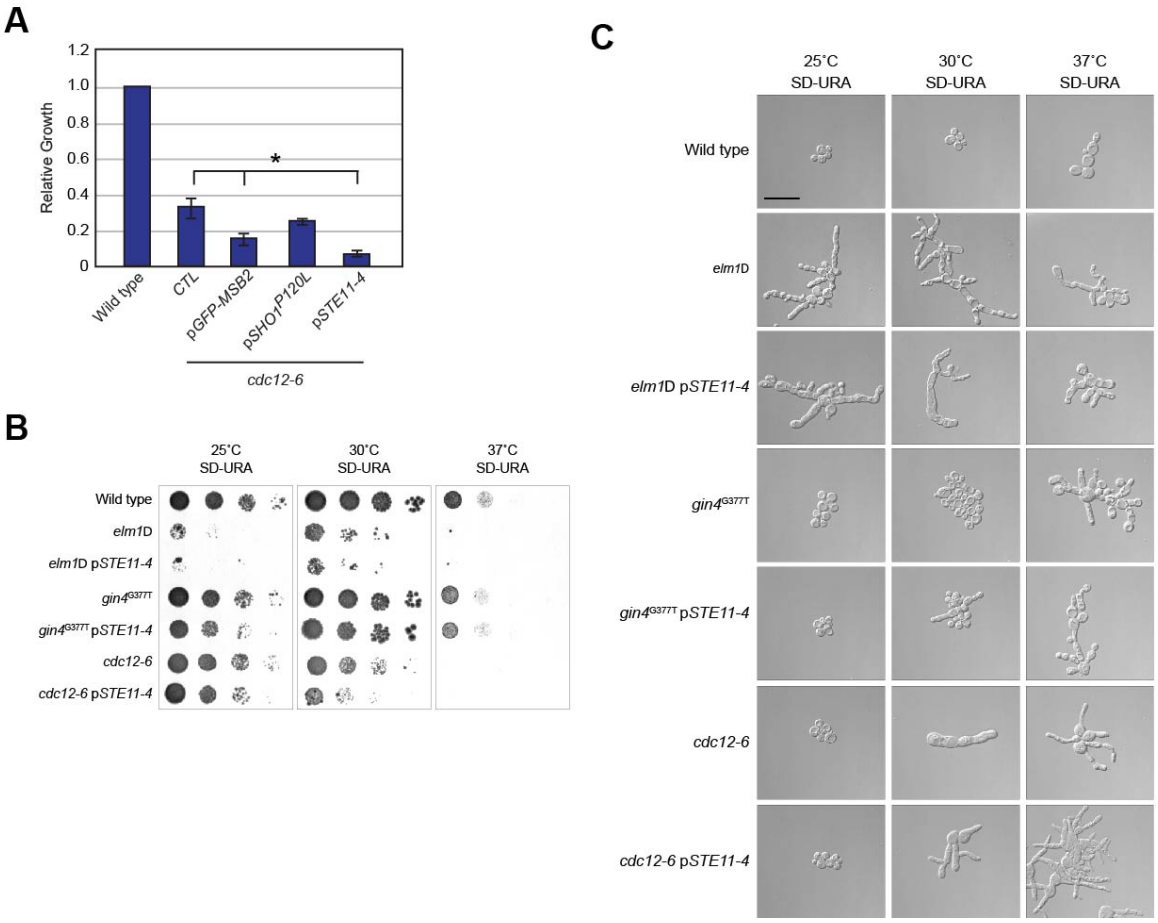

Figure S2. The fMAPK pathway does not rescue growth defects of the septin protein, Cdc12p and septin organizing kinases, Elm1p and Gin4p. (A) Growth assay of the *cdc12-6* mutant harboring indicated plasmids at 30°C. Asterisk, p-value <0.05. (**B**) Growth assay of indicated strains. Cells were spotted in serial dilutions on SD-URA semi-solid agar media and incubated at indicated temperatures for 3d. (**C**) Micrographs of cells from panel B. Bar, 20 microns.

Fig._S3

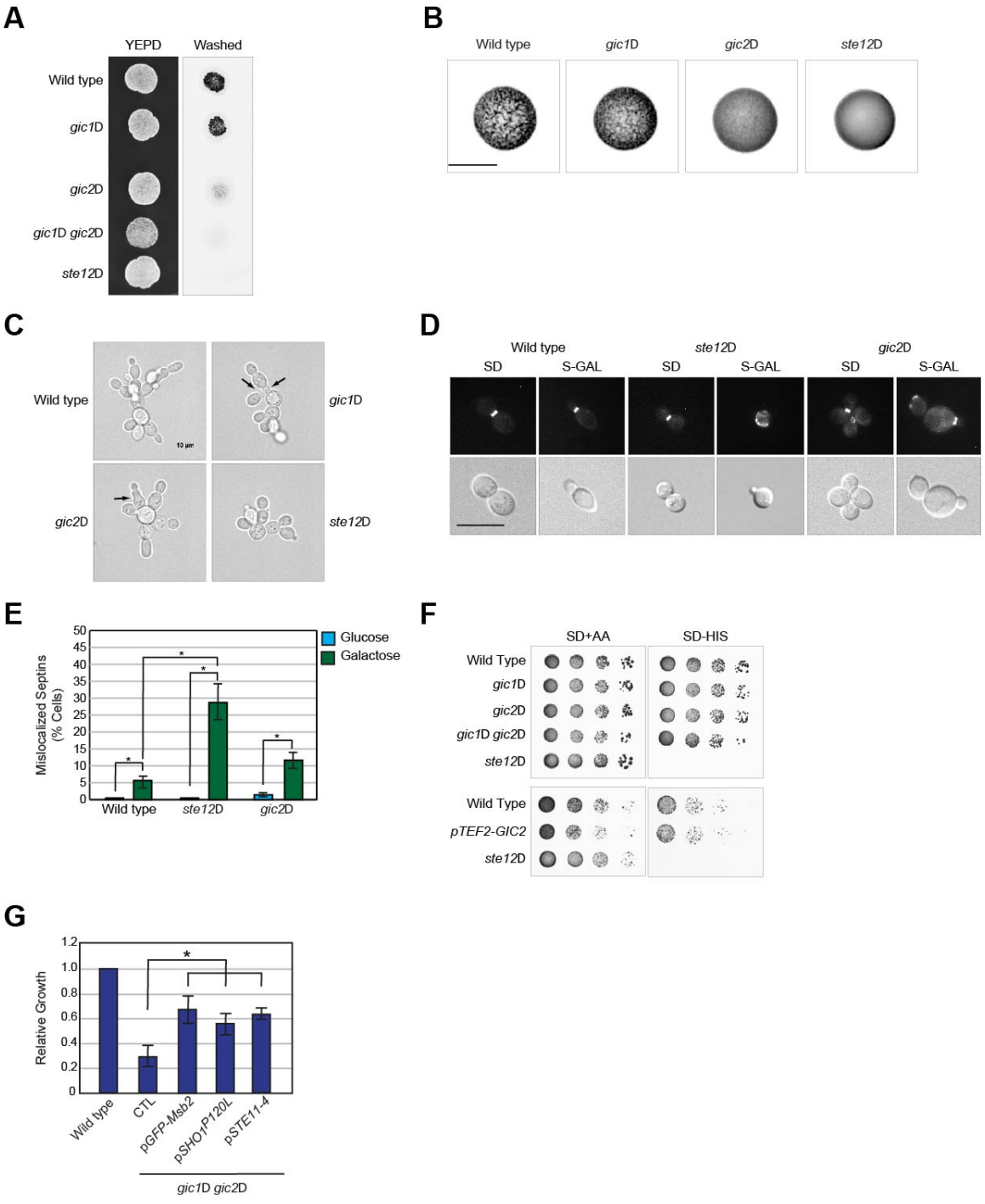

Figure S3. Role of Gic2p in regulating filamentous growth. (A) Invasive growth of the indicated strains by the PWA. Equal concentrations of cells were spotted onto YEPD media for 48 h. **(B)** Colony morphology for wild type, *gic1*Δ, *gic2*Δ and *ste12*Δ mutants. Equal concentrations of cells were spotted onto YEP-GAL medium for 24 h. Bar, 1 cm.

(C) Cell morphology for wild type, *gic1*Δ, *gic2*Δ and *ste12*Δ mutants by the single cell invasive growth assay. Arrows indicate morphological defects. Bar, 10 microns. **(D)** Cdc12p-GFP localization in wild type, *ste12*Δ and *gic2*Δ mutants on SD and S-GAL media at 30°C. **(E)** Quantitation of septin localization. 50 cells were counted in each trial for three separate trials. Error bars represent standard error of mean. Asterisk, p-value <0.05. (**F**) The *gic1*Δ and *gic2*Δ mutant combinations (top) and Gic2p overexpression (bottom) along with controls were evaluated for the fMAPK pathway activity using *FUS1*- *HIS3* reporter assay (McCaffrey et al., 1987). Cells were spotted in serial dilutions and incubated on selective media at 30°C for 2d. (**G**) Role of hyperactive fMAPK pathway alleles on the growth defect of *gic1*Δ *gic2*Δ double mutant at 37°C alongside controls. Asterisk, p-value < 0.05. CTL, plasmid pRS316.

Fig._S4

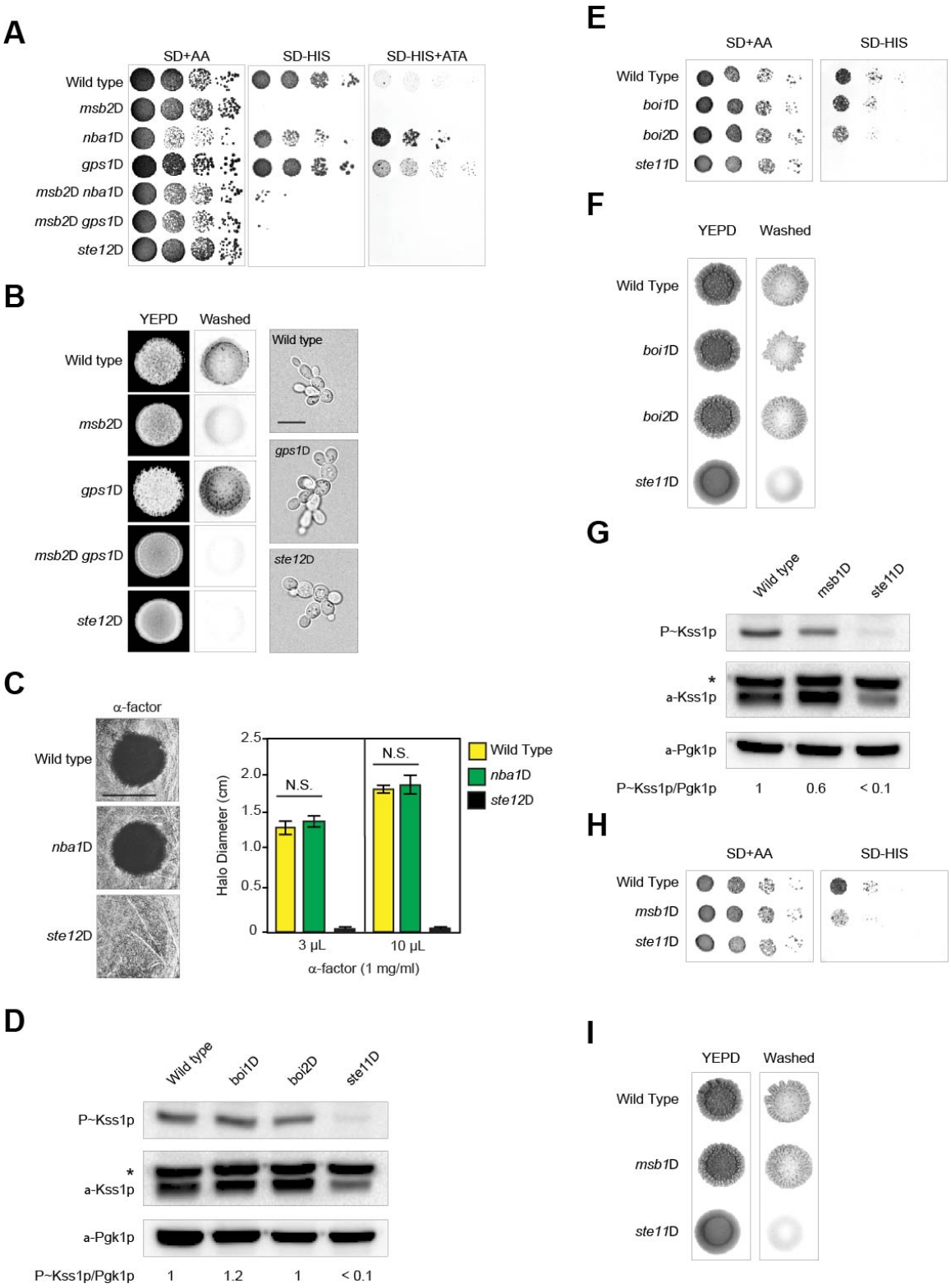

Figure S4. Role of Cdc42p-interacting proteins on the activity of the fMAPK pathway. (**A**) The fMAPK pathway activity was compared among wild type and mutants in isogenic background using *FUS1- HIS3* reporter assay. Cells were spotted in serial dilutions and incubated on selective media at 30°C for 3d. (**B**) The *gps1*Δ mutant alongside controls was examined for invasive growth by the PWA (left) and single cell invasive growth assay (right). For the PWA, cells were spotted for 48 h on YEPD. The plate was photographed, then washed in a stream of water and photographed again. For the single cell assay, cells were spread onto S-Glu media for 16h. Bar, 10 microns. (**C**) At left, halo assay. Cells (A_{600} 0.1) were spread on YEPD media and allowed to dry. 3 and 10 µl drops of 1mg/ml α-factor were applied to plates. Plates were incubated at 30°C and photographed at 24 h. The Bar, 1 cm. Representative image for 3 µl drop is shown. At right, halo diameters (cm) at 3 and 10 µl α-factor were measured by ImageJ. Error bars represent standard deviation among 3 independent trials. N.S., not significant. (**D**) Immunoblot analysis of wild type, *boi1*Δ, *boi2*Δ and *ste11*Δ to assess fMAPK pathway activity. Asterisk, non-specific band. Pgk1p, loading control. Numbers refer to the ratio of P~Kss1p to Pgk1p relative to wild type, set to 1. (**E**) Evaluation of the fMAPK pathway activity using *FUS1- HIS3* reporter assay in the indicated strains. Cells were spotted in serial dilutions and incubated at 30°C for 3 d. (**F**) Wild type, *boi1*Δ, *boi2*Δ and *ste11*Δ were evaluated for invasive growth using the PWA assay. (**G**) Immunoblot analysis of wild type, *msb1*Δ and *ste11*Δ to assess fMAPK pathway activity. See panel D for details. (**H**) Wild type, *msb1*Δ and *ste11*Δ were evaluated for fMAPK pathway activity using *FUS1- HIS3* reporter assay. See panel E for details. (**I**) PWA for indicated strains. See panel G for details.

Fig._S5

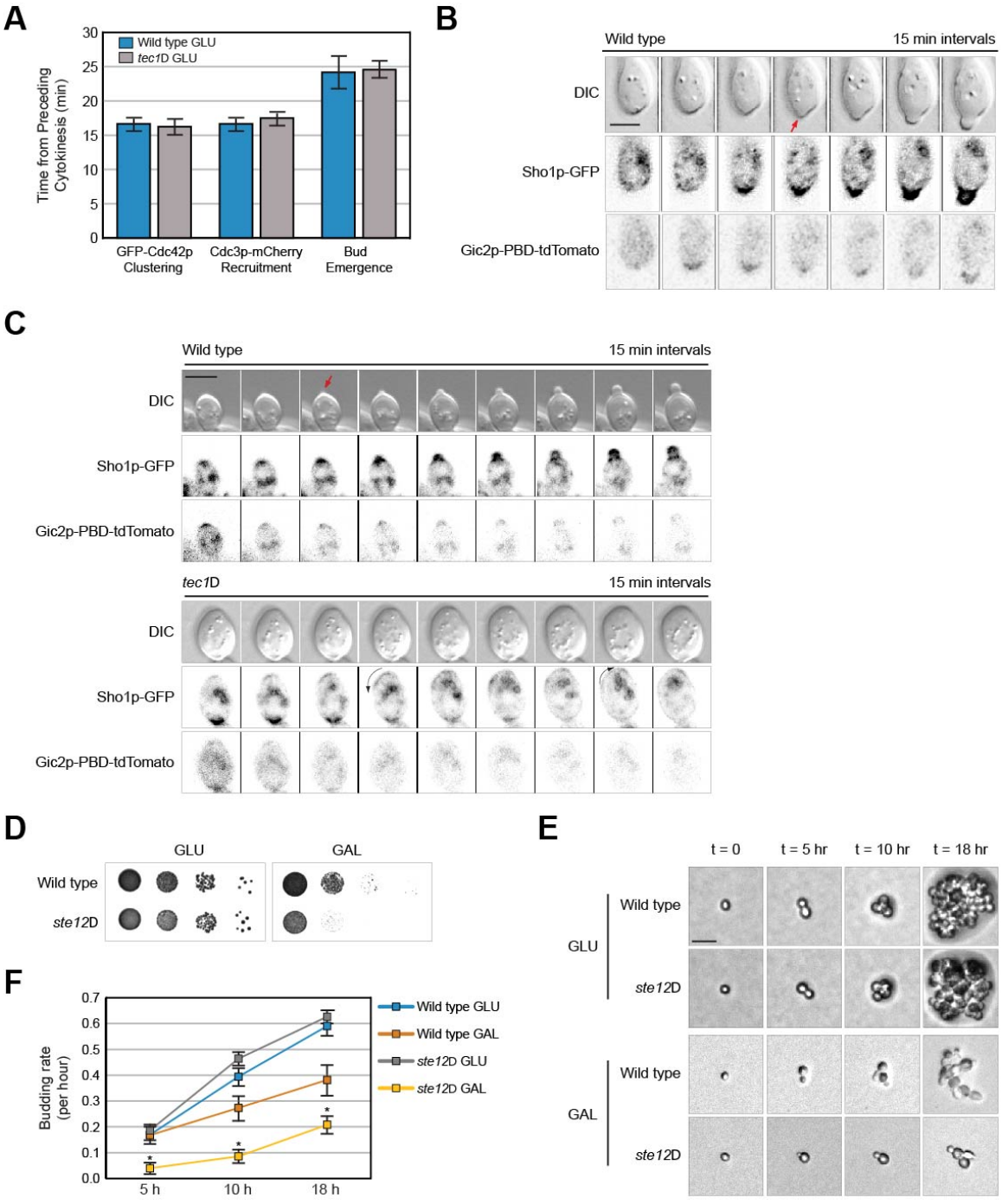

Figure S5. The fMAPK pathway mutant has growth defect under nutrient limiting conditions. (**A**) Quantitation of the timing of GFP-Cdc42p clustering, Cdc3p-mCherry recruitment and bud emergence in wild-type cells (n=6) and *tec1*Δ cells (n=12) grown on semi-solid SD-URA media. Error bar represent standard error of mean. (**B**) Co-

localization of Sho1p-GFP and Gic2p-PBD-tdTomato in wild-type cells grown in galactose for the indicated times at 15 min intervals. Red Arrow, bud emergence. Bar, 5 microns. (**C**) Same as B, except a representative example of wild type and *tec1*Δ mutant is shown. Black arrows, wandering Sho1p-GFP along the distal pole. (**D**) Growth assay of wild type and the *ste12*Δ mutant in glucose (GLU) and galactose (GAL). (**E**) Time series of single cell assay on wild-type cells and the *ste12*Δ mutant in GLU and GAL. Bar, 20 microns. (**F**) Quantification of budding rate of cells in panel E. Budding rate was calculated as described in Materials and Methods. Error bars, standard error of mean from 30 cells. Asterisk, p-value <0.05.

Fig._S6

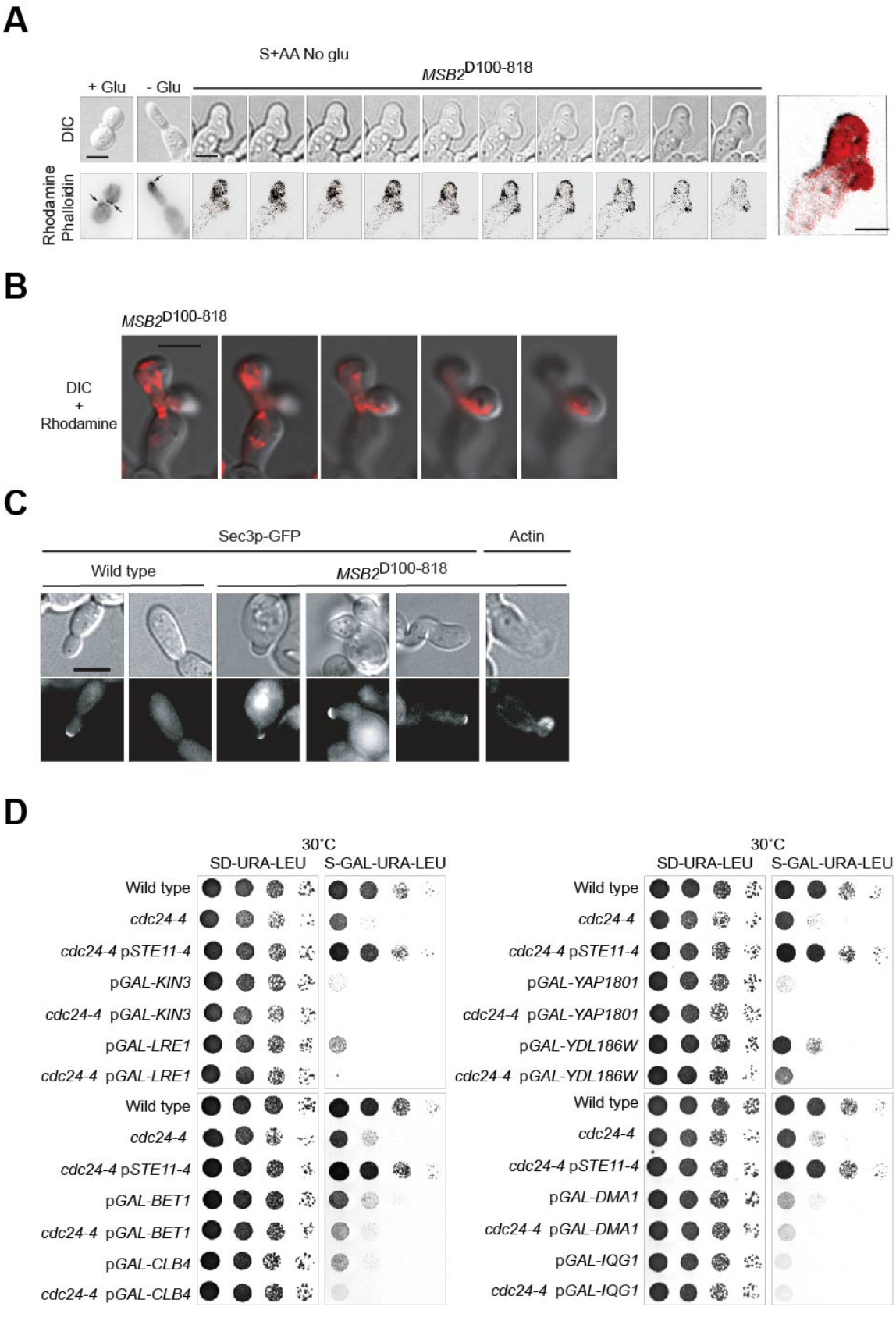

Figure S6. Multiple growth sites by the fMAPK pathway. (**A**) At left, actin staining of cells by rhodamine phalloidin. Bar, 5 microns. Micrographs for *MSB2*$^{\Delta 100\text{-}818}$ shown at different focal planes in the Z-axis. At right, inverted maximum intensity projection of cell on left shown using red lookup table. (**B**) Merged image of DIC and rhodamine phalloidin staining of a cell expressing *MSB2*$^{\Delta 100\text{-}818}$. Serial sections in the plane of the Z-axis are shown. Bar, 5 microns. (**BC**) At left, wild type and *MSB2*$^{\Delta 100\text{-}818}$ expressing Sec3p-GFP evaluated by single cell assay. At right, rhodamine phalloidin staining of a cell expressing Msb2p$^{\Delta 100\text{-}818}$. (**D**) Wild-type cells and the *cdc24-4* mutant containing the indicated plasmids (Gelperin et al., 2005) were spotted in serial dilutions onto SD-URA-LEU (GLU) and S-GAL-URA-LEU (GAL) media and incubated at 30°C for 2 d.

Table S1. Yeast strains used in the study

Name	Genotype	Reference
PC301[a]	MATa *ura3-52 ste12*::*URA3*	Cullen and Sprague, 2002
PC313	MATa *ura3-52*	Liu et al., 1993
PC538	MATa *ste4 FUS1-lacZ FUS1-HIS3 ura3-52*	Cullen et al., 2004
PC539	MATa *ste4 FUS1-lacZ FUS1-HIS3 ura3-52 ste12*::*URA3*	Cullen et al., 2004
PC544	MATa *ste4 FUS1-lacZ FUS1-HIS3 ura3-52 bni1*::*KlURA3*[b]	Cullen and Sprague, 2002
PC611	MATa *ste4 FUS1-lacZ FUS1-HIS3 ura3-52 ste11*::*KlURA3*	Cullen et al., 2004
PC622	MATa *ste4 FUS1-lacZ FUS1-HIS3 ura3-52 GAL-SHO1*::*KanMX6*	Cullen et al., 2004
PC948	MATa *ste4 FUS1-lacZ FUS1-HIS3 ura3-52 msb2*::*KanMX6*	Cullen et al., 2004
PC1052	MATa *ste4 FUS1-lacZ FUS1-HIS3 ura3-52 GAL-SHO1*::*KanMX6 ste11*::*KlURA3*	This study
PC1057	MATa *ste4 FUS1-lacZ FUS1-HIS3 ura3-52 ste11*::*URA3*	Cullen and Sprague, 2002
PC1205	MATa *ste4 FUS1-lacZ FUS1-HIS3 ura3-52 CDC24-GFP*::*KanMX6*	Vadaie et al., 2008
PC1512	MATa *ste4 FUS1-lacZ FUS1-HIS3 ura3-52 CDC24-GFP*::*KanMX6 MSB2-HA*$^{\Delta 100-818}$	This study
PC1516	MATa *ste4 FUS1-lacZ FUS1-HIS3 ura3-52 MSB2-HA*$^{\Delta 100-818}$	Cullen et al., 2004
PC1653	MATa *ste4 FUS1-lacZ FUS1-HIS3 ura3-52 CDC24-GFP::HYG GAL-SHO1*::*KanMX6*	This study
PC1661	NY64 MATa *ura3-52 sec15-1*	Finger and Novick, 2000
PC1806	MATa *ste4 FUS1-lacZ FUS1-HIS3 ura3-52 GAL-MSB2-HA*$^{\Delta 100-818}$::*KanMX6*	This study
PC1811	MATa *ste4 FUS1-lacZ FUS1-HIS3 ura3-52 MSB2-HA*$^{\Delta 100-818}$ *ste12*::*URA3*	Vadaie et al., 2008

Name	Genotype	Reference
PC1837	MATa *ste4 FUS1-lacZ FUS1-HIS3 ura3-52 GAL-MSB2-HA*$^{\Delta 100\text{-}818}$*::KanMX6 ste12::KlURA3*	This study
PC1866	MATa *ste4 FUS1-lacZ FUS1-HIS3 ura3-52 ABP140-YFP::KanMX6*	Pitoniak et al., 2009
PC1890	MATa *ste4 FUS1-lacZ FUS1-HIS3 ura3-52 GAL-MSB2-HA::NAT GAL-SHO1::HYG ABP140-YFP::KanMX6*	This study
PC1894	MATa *ste4 FUS1-lacZ FUS1-HIS3 ura3-52 leu2::HYG*	Vadaie et al., 2008
PC2538	MATa *ste4 FUS1-lacZ FUS1-HIS3 ura3-52 leu2::HYG STE11-4::URA3*	Chavel et al., 2010
PC2710	MATa *ste4 FUS1-lacZ FUS1-HIS3 ura3-52 cdc12-6::NAT*	Basu et al., 2016
PC2744	MATa *ste4 FUS1-lacZ FUS1-HIS3 ura3-52 CLB2-HA*	This study
PC3497	MATa *ste4 FUS1-lacZ FUS1-HIS3 ura3-52MSB2-HA*@500 aa *msb1::KlURA3*	Pitoniak et al., 2015
PC3756	MATa *ste4 FUS1-lacZ FUS1-HIS3 ura3-52 boi1::KlURA3*	Pitoniak et al., 2015
PC3758	MATa *ste4 FUS1-lacZ FUS1-HIS3 ura3-52 boi2::KlURA3*	Pitoniak et al., 2015
PC4248	MATa *ste4 FUS1-lacZ FUS1-HIS3 ura3-52 rax2::KanMX6*	Basu et al., 2016
PC6050	MATa *ste4 FUS1-lacZ FUS1-HIS3 ura3-52 elm1::HYG*	Adhikari and Cullen, 2014
PC6077	MATa *ste4 FUS1-lacZ FUS1-HIS3 ura3-52 leu2::HYG cdc24::NAT* pRS315 *cdc24-4*	Pitoniak et al., 2015
PC6627	MATa *ura3-52* Yip211 *GIC2-PBD*-tdTomato	Basu et al., 2020
PC6810	*MAT***a** *ura3-52 leu2 ssk1*	Basu et al., 2020
PC6932	MATa *ste4 FUS1-lacZ FUS1-HIS3 ura3-52 gps1::KlURA3*	This study
PC6936	MATa *ste4 FUS1-lacZ FUS1-HIS3 ura3-52 leu2::HYG cdc24* pRS315 *cdc24-4*	This study
PC6955	MATa *ste4 FUS1-lacZ FUS1-HIS3 ura3-52 gin4*^{G377T}	Chow et al., 2019
PC6958	MATa *ste4 FUS1-lacZ FUS1-HIS3 ura3-52 leu2::HYG cdc24* pRS315 *cdc24-4 ste12::NAT*	This study

Name	Genotype	Reference
PC6969	MATa *ste4 FUS1-lacZ FUS1-HIS3 ura3-52 leu2*::*HYG cdc24* pRS315 *cdc24-4 cln1*::*NAT*	This study
PC7000	MATa *ste4 FUS1-lacZ FUS1-HIS3 ura3-52 msb2*::*KanMX6 nba1*::*KlURA3*	This study
PC7002	MATa *ste4 FUS1-lacZ FUS1-HIS3 ura3-52 msb2*::*KanMX6 gps1*::*KlURA3*	This study
PC7012	MATa *ste4 FUS1-lacZ FUS1-HIS3 ura3-52 leu2*::*HYG cdc24* pRS315 *cdc24-4 rsr1*::*NAT*	This study
PC7018	MATa *ste4 FUS1-lacZ FUS1-HIS3 ura3-52 leu2*::*HYG cdc24* pRS315 *cdc24-4 bni1*::*NAT*	This study
PC7020	MATa *ste4 FUS1-lacZ FUS1-HIS3 ura3-52 leu2*::*HYG cdc24* pRS315 *cdc24-4 pbs2*::*NAT*	This study
PC7022	MATa *ste4 FUS1-lacZ FUS1-HIS3 ura3-52 leu2*::*HYG cdc24* pRS315 *cdc24-4 bud8*::*NAT*	This study
PC7034	MATa *ste4 FUS1-lacZ FUS1-HIS3 ura3-52 gic1*::*KanMX6*	This study
PC7036	MATa *ste4 FUS1-lacZ FUS1-HIS3 ura3-52 leu2*::*HYG cdc24* pRS315 *cdc24-4 gic2*::*NAT*	This study
PC7040	MATa *ste4 FUS1-lacZ FUS1-HIS3 ura3-52 leu2*::*HYG cdc24* pRS315 *cdc24-4 bud4*::*NAT*	This study
PC7043	MATa *ste4 FUS1-lacZ FUS1-HIS3 ura3-52 gic2*::*NAT*	This study
PC7044	MATa *ste4 FUS1-lacZ FUS1-HIS3 ura3-52 gic1*::*KanMX6 gic2*::*NAT*	This study
PC7046	MATa *ste4 FUS1-lacZ FUS1-HIS3 ura3-52 nba1*::*KanMX6*	This study
PC7050	MATa *ura3-52 nba1*::*KanMX6*	This study
PC7122	MATa *ste4 FUS1-lacZ FUS1-HIS3 ura3-52 leu2*::*HYG cdc24* pRS315 *cdc24-4 flo11*::*NAT*	This study
PC7123	MATa *ste4 FUS1-lacZ FUS1-HIS3 ura3-52 gps1*::*KanMX6*	
PC7148	MATa *ste4 FUS1-lacZ FUS1-HIS3 ura3-52 leu2*::*HYG cdc24* pRS315 *cdc24-4 tec1*::*NAT*	This study

Name	Genotype	Reference
PC7320	MATa *ura3-52* Yip211 *GIC2-PBD*-tdTomato *tec1*::*NAT*	This study
PC7365	MATa *ura3-52 CDC3-mCherry*::*HYG*	This study
PC7366	MATa *ura3-52 CDC3-mCherry*::*HYG ste12*::*NAT*	This study
PC7367	MATa *ura3-52 CDC3-mCherry*::*HYG tec1*::*NAT*	This study
PCV36T	*MAT***a** *ura3-52 leu2 ssk1 CDC42*^{V36T}	Basu et al., 2020

[a]All strains are Σ1278b background unless otherwise indicated. [b]Kl, *Kluyveromyces lactis*.

Table S2. Plasmids used in the study[a]

Name	Description	Reference
PC187	YCp50-*STE4* CEN/URA3	Stevenson et al., 1992
PC1333	YCp50-*STE11-4*	Stevenson et al., 1992
PC1365	YCplac181 *CDC12-GFP*	Fares et al., 1996
PC1665	p*SEC3-GFP*	Finger and Novick, 1997
PC1696	p*GFP-MSB2*	Vadaie et al., 2008
PC1715	pRS316-*SHO1*$^{D16H\ P120L}$-*GFP*	Vadaie et al., 2008
PC1885	pMPY-3xHA	Schneider et al., 1995
PC1964	pRS316-*SHO1*^{D16H}-*GFP*	Marles et al., 2004
PC2151	pRS315	Sikorski and Hieter, 1989
PC2205	pNAT	Goldstein and McCusker, 1999
PC2206	pHYG	Goldstein and McCusker, 1999
PC2207	pRS316	Sikorski and Hieter, 1989
PC6365	YEp352-*TEF2*	Pitoniak et al., 2015
PC6454	pRS316-*GFP*-linker-*CDC42*	Basu et al., 2020
PC6626	Yip211 *GIC2-PBD*-tdTomato	Okada et al., 2013

Name	Description	Reference
PC7082	YEp352-*TEF2-GIC2*	This study
PC7137	pRS316- p*ACT1-EGFP-CRIBCLA4-CDC42*$^{\Delta CAAX}$*-mCherry-CAAX*	Smith et al., 2013
PC7138	pRS316- p*ACT1-EGFP-CRIBCLA4-CDC42*$^{Q61L\Delta CAAX}$*-mCherry-CAAX*	Smith et al., 2013
PC7139	pRS316- p*ACT1-EGFP-CRIBCLA4-CDC42*$^{D57Y\Delta CAAX}$*-mCherry-CAAX*	Smith et al., 2013
PC7143	YCplac181 *CDC12-GFP*::*KanMX6*	This study
PC7150	YCplac181 *CDC12-GFP*::*NAT*	This study
PC7340	pRS316-*GFP*-linker-*CDC42*::*KanMX6*	This study
PC7357	pRS316-*GFP*-linker-*CDC42*::*NAT*	This study
PC7359	pRS316-p*ACT1-EGFP-CRIBCLA4-CDC42*$^{\Delta CAAX}$*-mCherry-CAAX*::*KanMX6*	This study
PC7361	pRS316-*SHO1*^{D16H}*-GFP*::*KanMX6*	This study
PC7363	pRS316-*SHO1*^{D16H}*-GFP*::*NAT*	This study
PC7381	pRS315 *cdc24-4*	Pitoniak et al., 2015

[a]The following plasmids were used from the movable ORF collection (Gelperin et al., 2005): pGAL-KIN3-HA, pGAL-LRE1-HA, pGAL-BET1-HA, pGAL-CLB4-HA, pGAL-YAP1801-HA, pGAL-YDL186W-HA, pGAL-DMA1-HA, pGAL-IQG1-HA and pGAL-STE7-HA.

SUPPLEMENTAL MOVIES

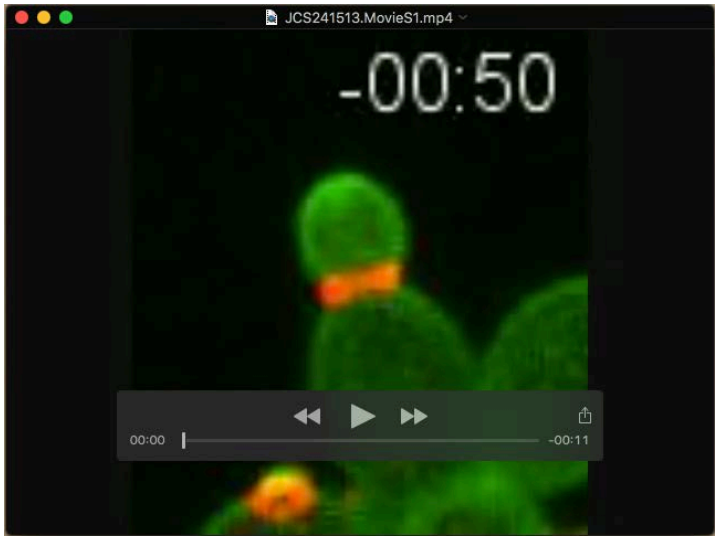

Movie 1. Time lapse of wild-type cells expressing GFP-Cdc42p and Cdc3p-mCherry in GAL. Time interval, 10 min. Time 0 is when septin hourglass splits into double ring marking cytokinesis.

Movie 2. Time lapse of*ste12*Δ mutant expressing GFP-Cdc42p and Cdc3p-mCherry in GAL. See movie 1 for details.

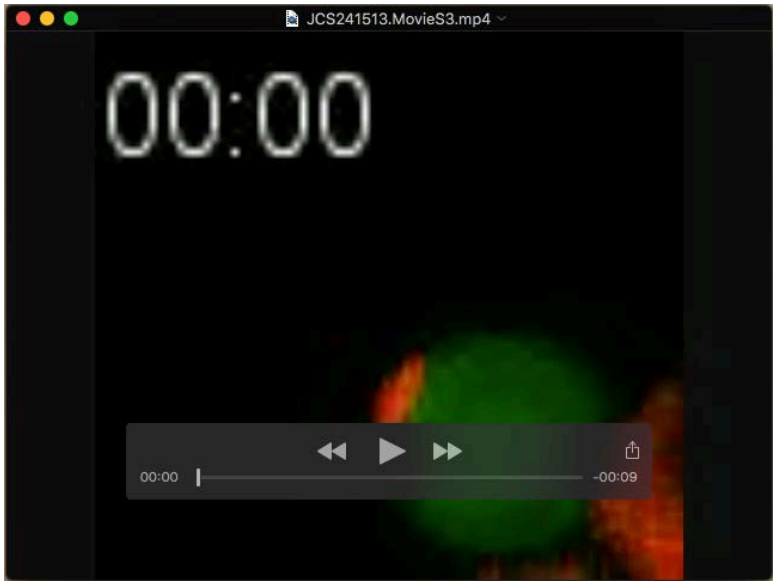

Movie 3. Second example of *ste12*Δ mutant expressing GFP-Cdc42p and Cdc3p-mCherry in GAL. Time 0 indicates start of experiment.

Movie 4. Third example of *ste12*Δ mutant showing merged DIC and Cdc3p-mCherry grown in GAL. See movie 1 for details.

Movie 5. Fourth example of *ste12*Δ mutant showing merged DIC and Cdc3p-mCherry grown in GAL. Time 0 indicates start of experiment.

Movie 6. Time lapse of *tec1*Δ mutant expressing GFP-Cdc42p and Cdc3p-mCherry in GAL. Time interval, 15 min. See movie 1 for details.

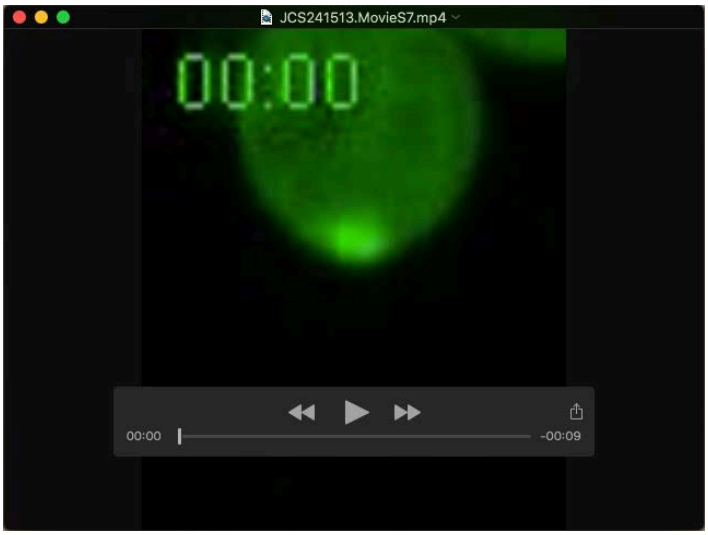

Movie 7. Time lapse of wild-type cells expressing GFP-Cdc42p. Time interval, 10 min.

Movie 8. Time lapse of *MSB2*$^{\Delta 100\text{-}818}$ expressing GFP-Cdc42p. Time interval, 20 min.